Parton distribution functions for the LHC era

Pavel Nadolsky
in collaboration with
Q.-H. Cao, J. Huston, H.-L. Lai, J. Pumplin,
D. Stump, W.-K. Tung, and C.-P. Yuan

Michigan State University

June 6, 2008

Global picture of QCD factorization

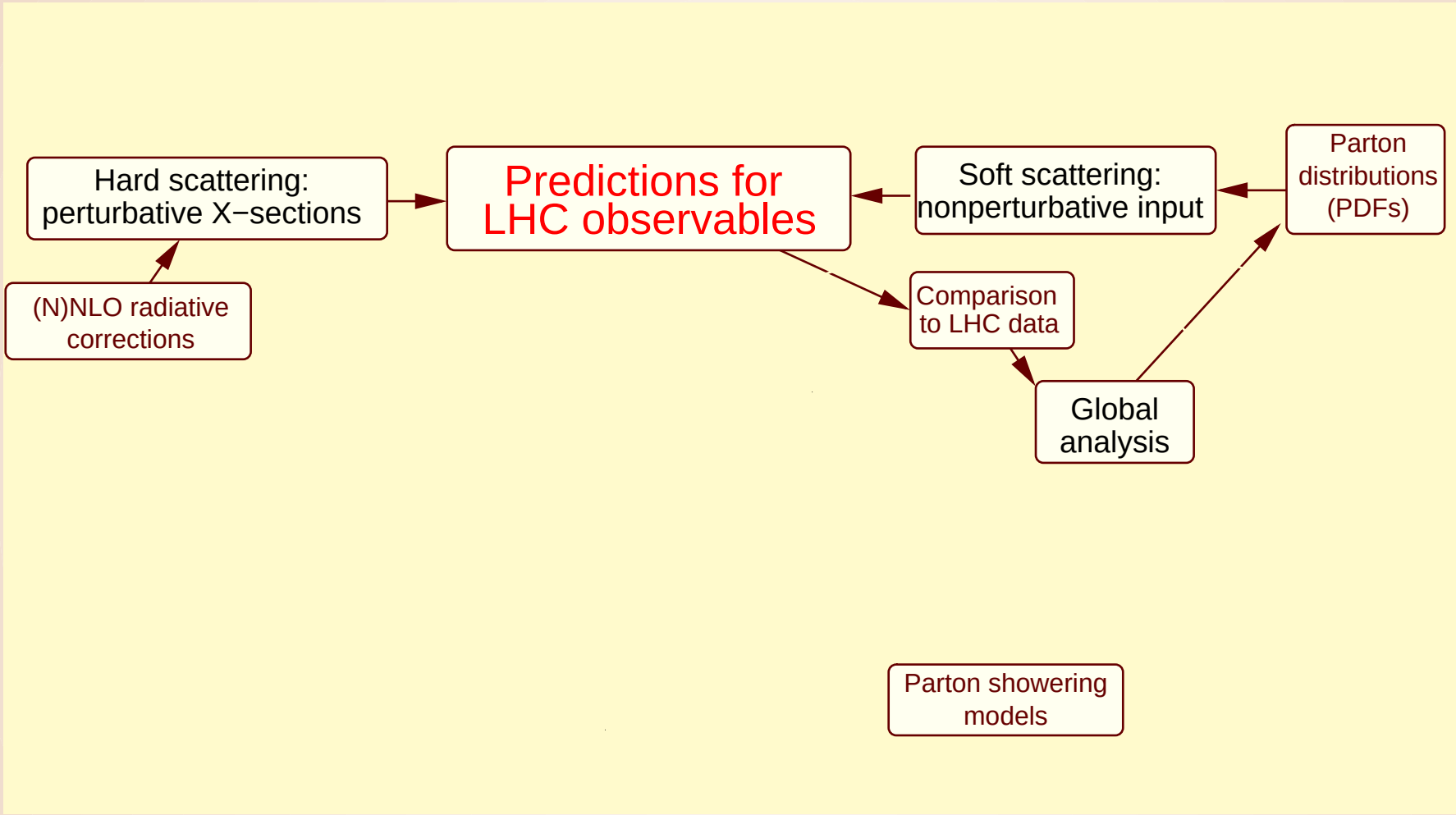

A relevant, yet incomplete, picture

Global picture of QCD factorization

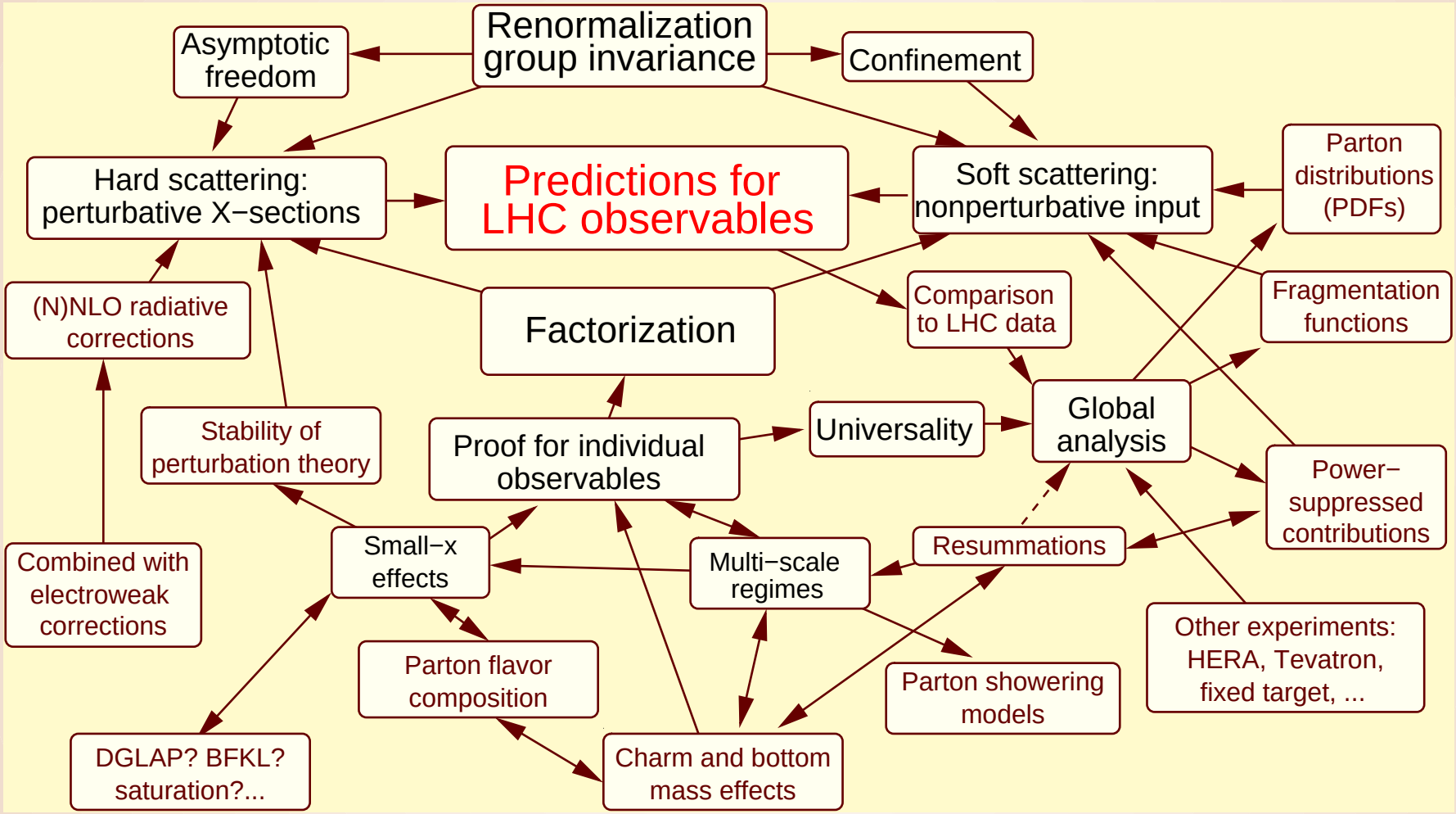

Global interconnections can be as important as (N)NLO perturbative contributions; are different at the LHC and Tevatron

Examples of global connections
(based on our recent studies)

- Heavy-quark mass effects on LHC W, Z cross sections
- PDF-induced correlations between physical observables
- Role of subleading channels (strangeness, intrinsic charm) in the PDF uncertainties

Extensive related work by other groups; see presentations at 2008 PDF4LHC, DIS, HERA-LHC workshops

A typical perturbative QCD calculation

Higgs boson production $pp \to (H \to \gamma\gamma)X$

A. Cross section $\sigma_{pp\to H\to\gamma\gamma}$ for production and decay of H, e.g. via $g + g \to H$

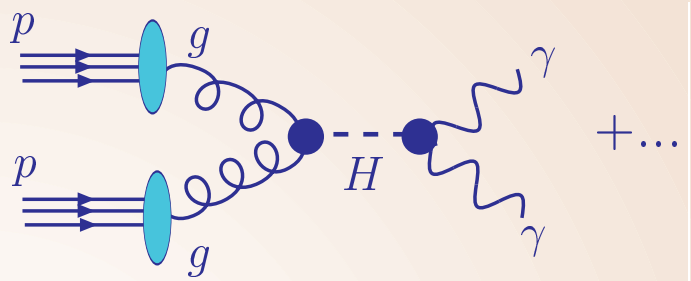

$$\sigma_{pp\to H\to\gamma\gamma} = \widehat{\sigma}_{gg\to H\to\gamma\gamma} f_{g/p}(x_1, M_H) f_{g/p}(x_2, M_H) + \ldots$$

- $\widehat{\sigma}_{gg\to H\to\gamma\gamma}$ is the hard-scattering cross section, given by a perturbation series in α_s **(at least formally)**
- $f_{g/p}(x,\mu)$ is the parton distribution function for finding a gluon g with momentum $x\vec{P}$ in a proton with momentum $\vec{P}$ ($\left|\vec{P}\right| \approx E \approx \mu > 1$ GeV) at a typical momentum μ

$f_{g/p}(x,\mu)$ are universal (process-independent) nonperturbative functions

Perturbative evolution of $f_{i/p}(x,\mu)$; global fits

At the initial momentum scale $Q_0 \sim 1$ GeV, the PDF's are parametrized as

$$f_{i/p}(x,Q_0) = a_0 x^{a_1}(1-x)^{a_2} F(a_3,a_4,...)$$

At $Q > Q_0$, $f_{i/p}(x,\mu)$ are computed by solving Dokshitzer-Gribov-Lipatov-Altarelli-Parisi (DGLAP) equations,

$$\mu \frac{df_{i/p}(x,\mu)}{d\mu} = \sum_{j=g,u,\bar{u},d,\bar{d},....} \int_x^1 \frac{dy}{y} P_{i/j}\left(\frac{x}{y},\alpha_s(\mu)\right) f_{j/p}(y,\mu),$$

with $P_{i/j}$ known to order α_s^3 (NNLO):

$$P_{i/j}(x,\alpha_s) = \alpha_s P_{i/j}^{(1)}(x) + \alpha_s^2 P_{i/j}^{(2)}(x) + \alpha_s^3 P_{i/j}^{(3)}(x) + ...$$

The values of a_i and their uncertainties are determined from a global fit to hadron scattering data

Global analysis at Michigan State/Taiwan/Washington

- a part of the Coordinated Theoretical Experimental study of QCD (CTEQ) in U.S.A.
- development of general-purpose PDF's

  (Wu-Ki Tung and collaborators)
- new CTEQ6.6M standard set and 44 extreme eigenvector sets *(arXiv:0802.0007)*
  - a fit of NLO cross sections to 2714 experimental data points from deep inelastic scattering, lepton pair (via γ^*, W) production, and Tevatron Run-1 jet production
  - improved treatment of s, c, b PDF's
  - correlation analysis of collider observables
  - available in the LHAPDF-5.4 library and at www.cteq.org

Multi-dimensional PDF error analysis

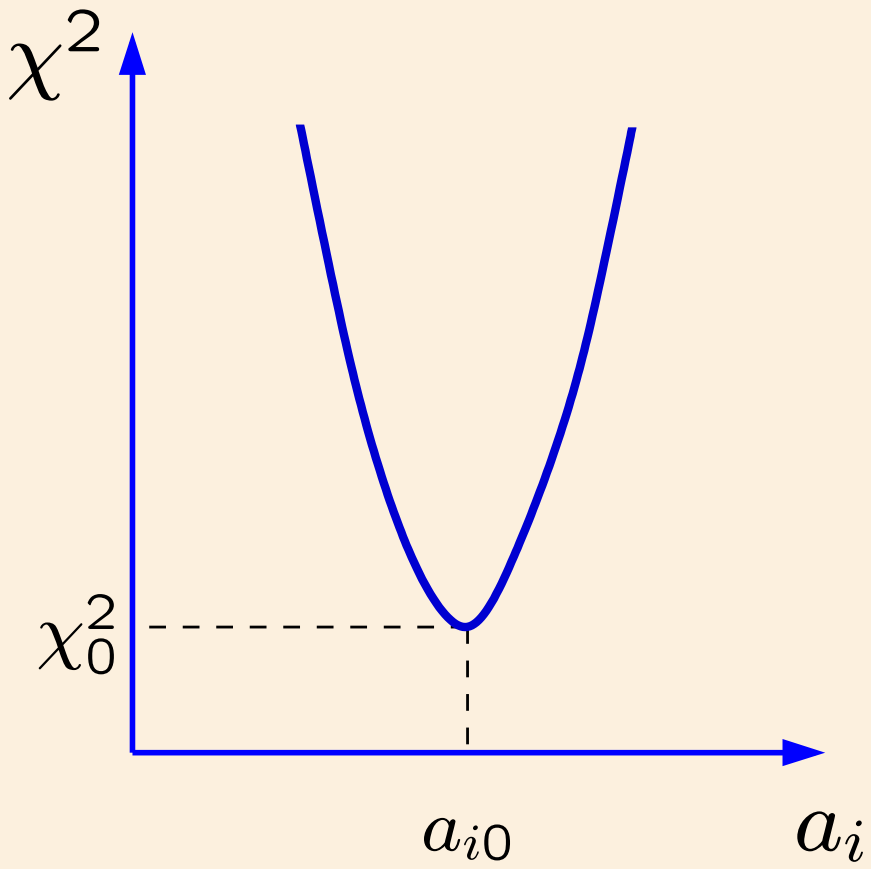

- Minimization of a likelihood function (χ^2) with respect to ~ 30 theoretical (mostly PDF) parameters $\{a_i\}$ and > 100 experimental systematical parameters
  - partly analytical and partly numerical

Multi-dimensional PDF error analysis

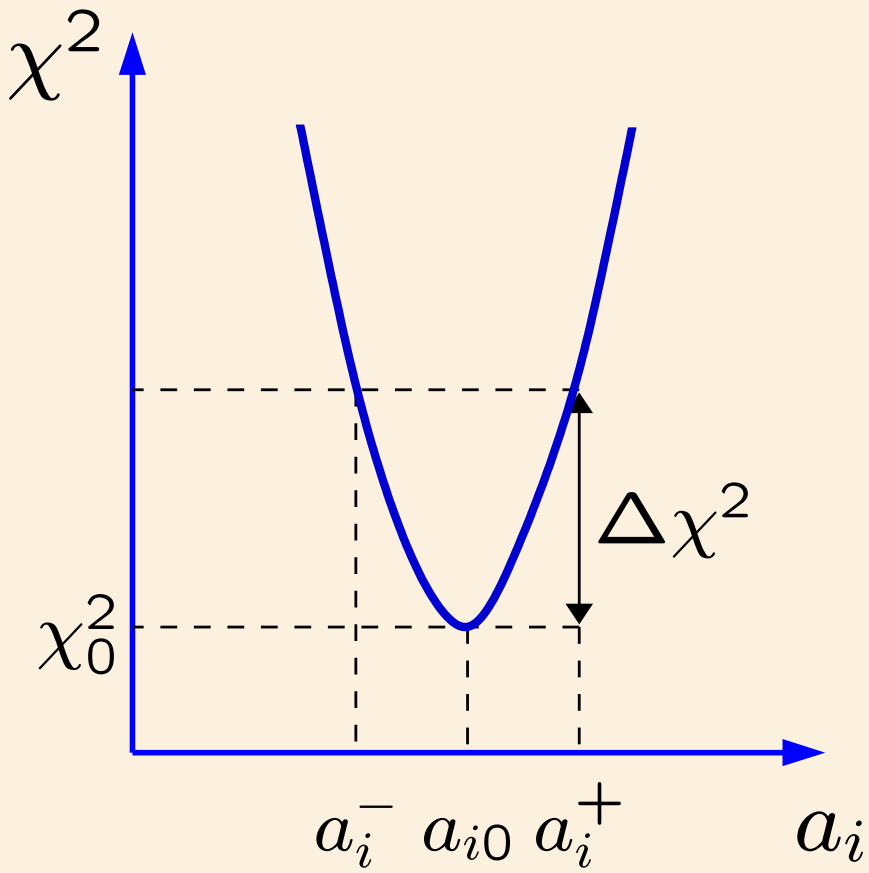

- Establish a confidence region for $\{a_i\}$ for a given tolerated increase in χ^2

Multi-dimensional PDF error analysis

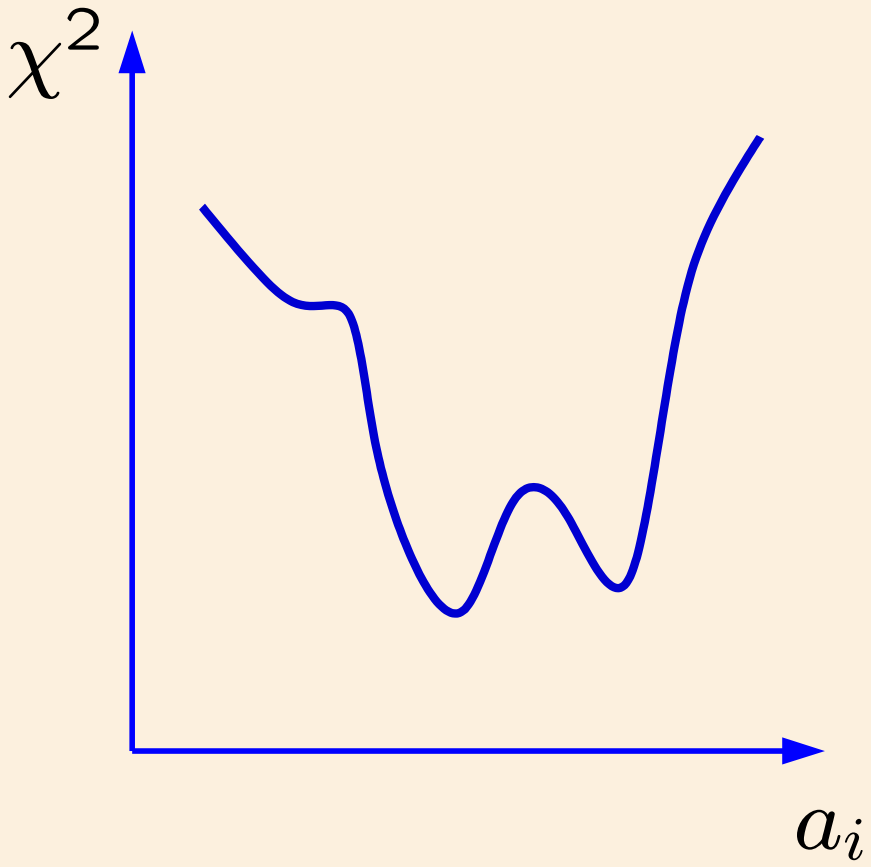

Pitfalls to avoid

- "Landscape"
  - disagreements between the experiments

In the worst situation, significant disagreements between M experimental data sets can produce up to $N \sim M!$ possible solutions for PDF's, with $N \sim 10^{500}$ reached for "only" about 200 data sets

Multi-dimensional PDF error analysis

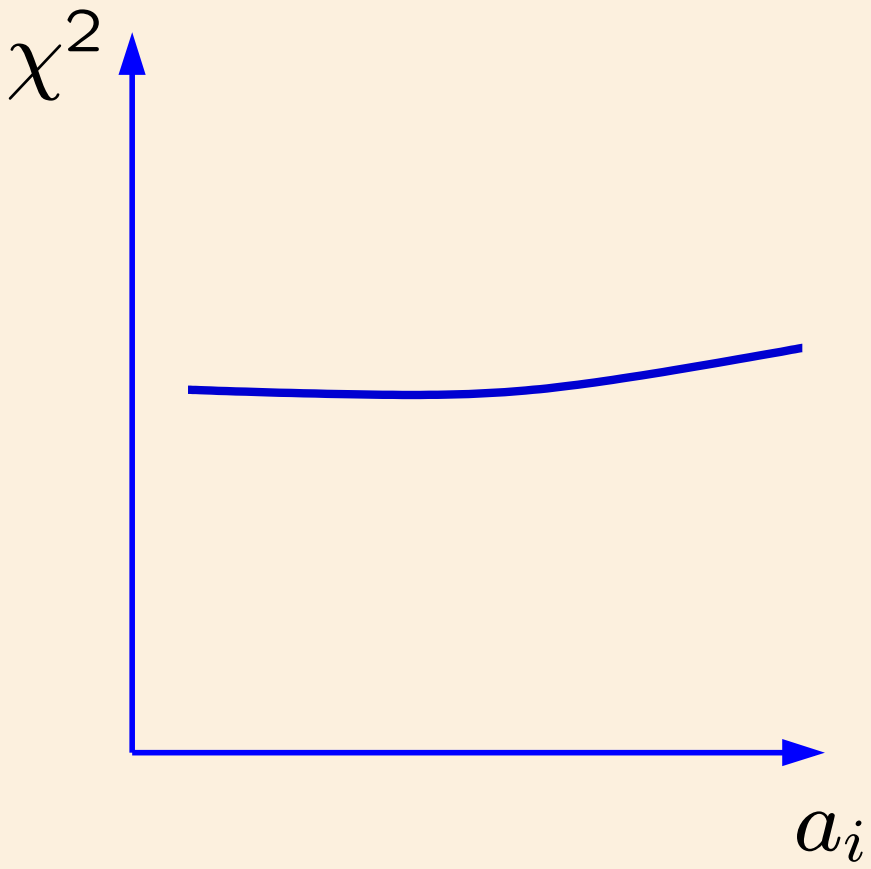

Pitfalls to avoid

- Flat directions
  - unconstrained combinations of PDF parameters
  - dependence on free theoretical parameters, especially in the PDF parametrization

Multi-dimensional PDF error analysis

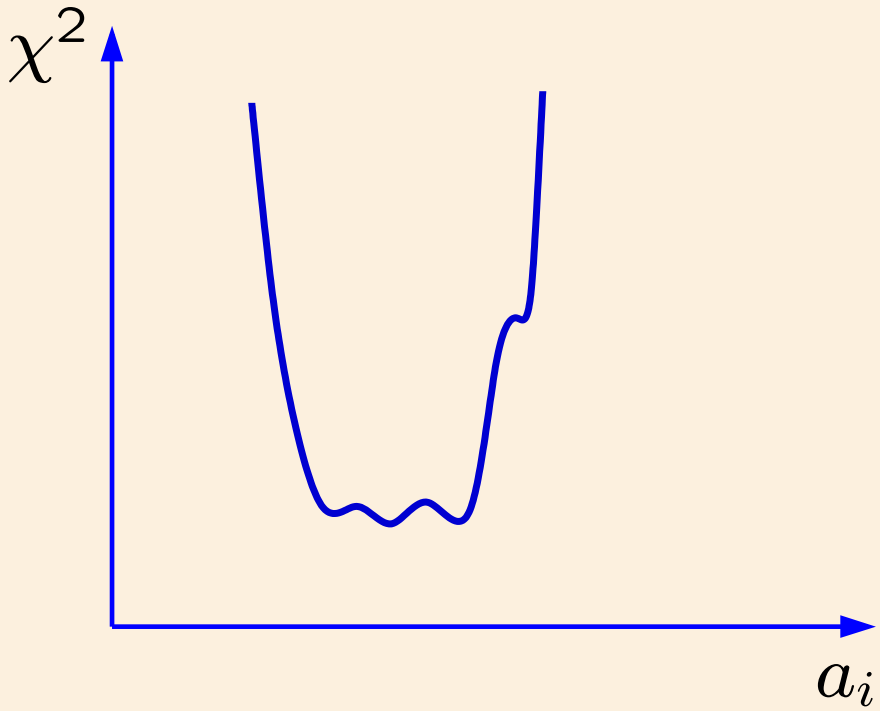

The actual χ^2 function shows

- a well pronounced global minimum χ^2_0
- weak tensions between data sets in the vicinity of χ^2_0 (mini-landscape)
- some dependence on assumptions about flat directions

Multi-dimensional PDF error analysis

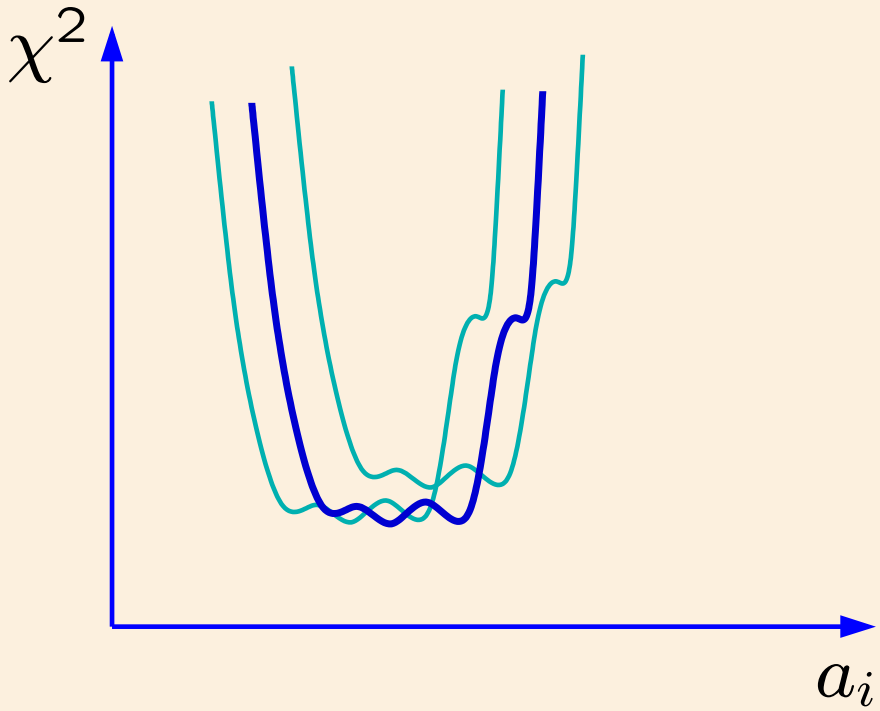

The actual χ^2 function shows

- a well pronounced global minimum χ^2_0
- weak tensions between data sets in the vicinity of χ^2_0 (mini-landscape)
- some dependence on assumptions about flat directions

Multi-dimensional PDF error analysis

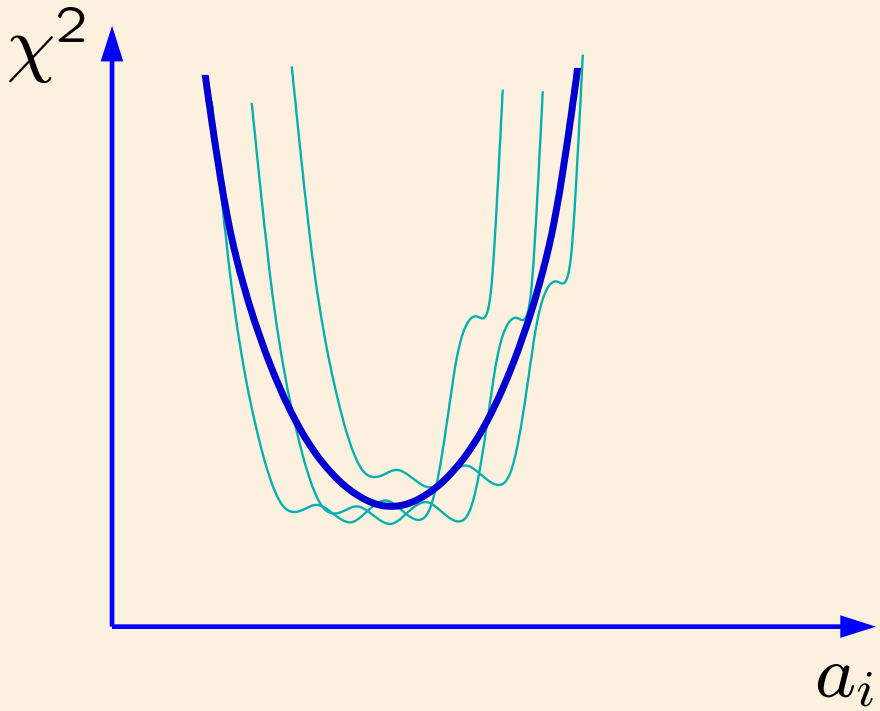

The actual χ^2 function shows

- a well pronounced global minimum χ^2_0
- weak tensions between data sets in the vicinity of χ^2_0 (mini-landscape)
- some dependence on assumptions about flat directions

The likelihood is approximately described by a quadratic χ^2 with a revised tolerance condition $\Delta\chi^2 \leq T^2$

Multi-dimensional PDF error analysis

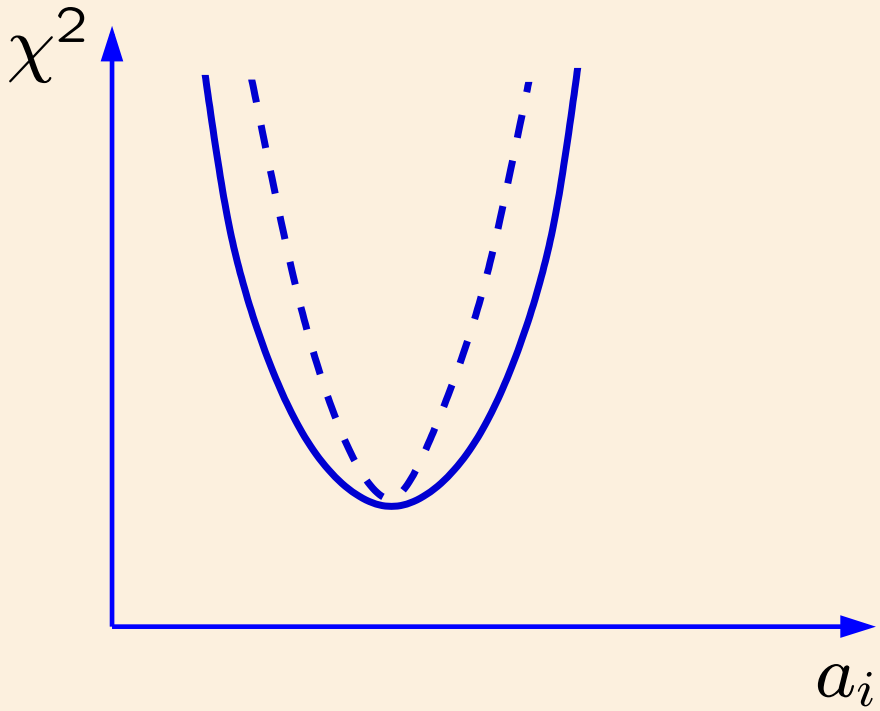

The actual χ^2 function shows

- a well pronounced global minimum χ^2_0
- weak tensions between data sets in the vicinity of χ^2_0 (mini-landscape)
- some dependence on assumptions about flat directions

The likelihood is approximately described by a quadratic χ^2 with a revised tolerance condition $\Delta\chi^2 \leq T^2$

Multi-dimensional PDF error analysis

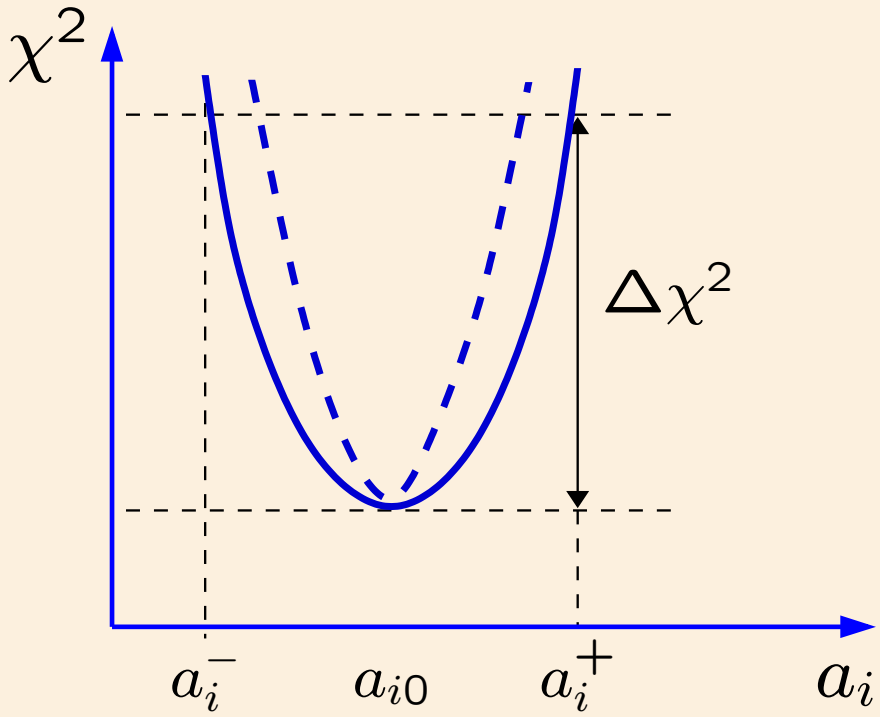

The actual χ^2 function shows

- a well pronounced global minimum χ^2_0
- weak tensions between data sets in the vicinity of χ^2_0 (mini-landscape)
- some dependence on assumptions about flat directions

The likelihood is approximately described by a quadratic χ^2 with a revised tolerance condition $\Delta\chi^2 \leq T^2$

CTEQ6 tolerance criterion (2001)

Acceptable values of PDF parameters must agree at ≈90% c.l. with all experiments included in the fit, *for a plausible range of assumptions about the PDF parametrization, scale dependence, experimental systematics, ...*

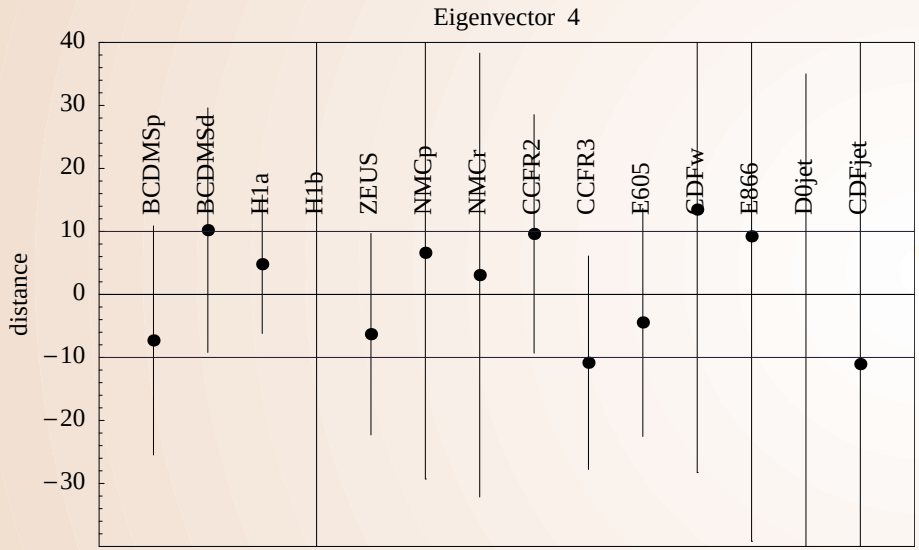

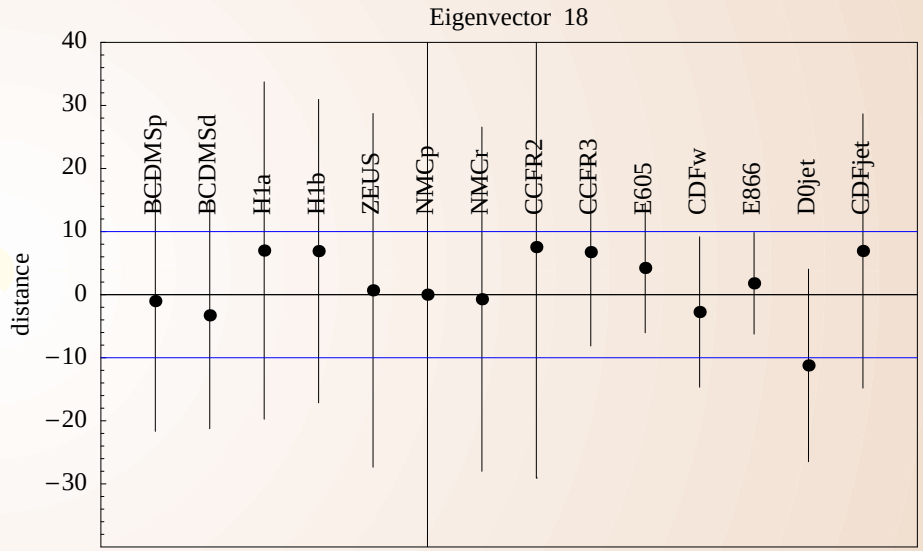

Can be crudely approximated (but does not have to) by assuming $T \approx 10$ for all PDF parameters

A somewhat stricter variant of this criterion is applied in the MSTW'08 analysis

HERAPDF0.1 set based on the combined neutral-current DIS data (2008)

The common fit of the combined data

Partons parametrized at $Q_0^2 = 4$ GeV^2 (Data Q^2>3.5 GeV^2)

Experimental+Model uncertainties taken into account

Errors of the fit estimated using $\Delta\chi^2$=1

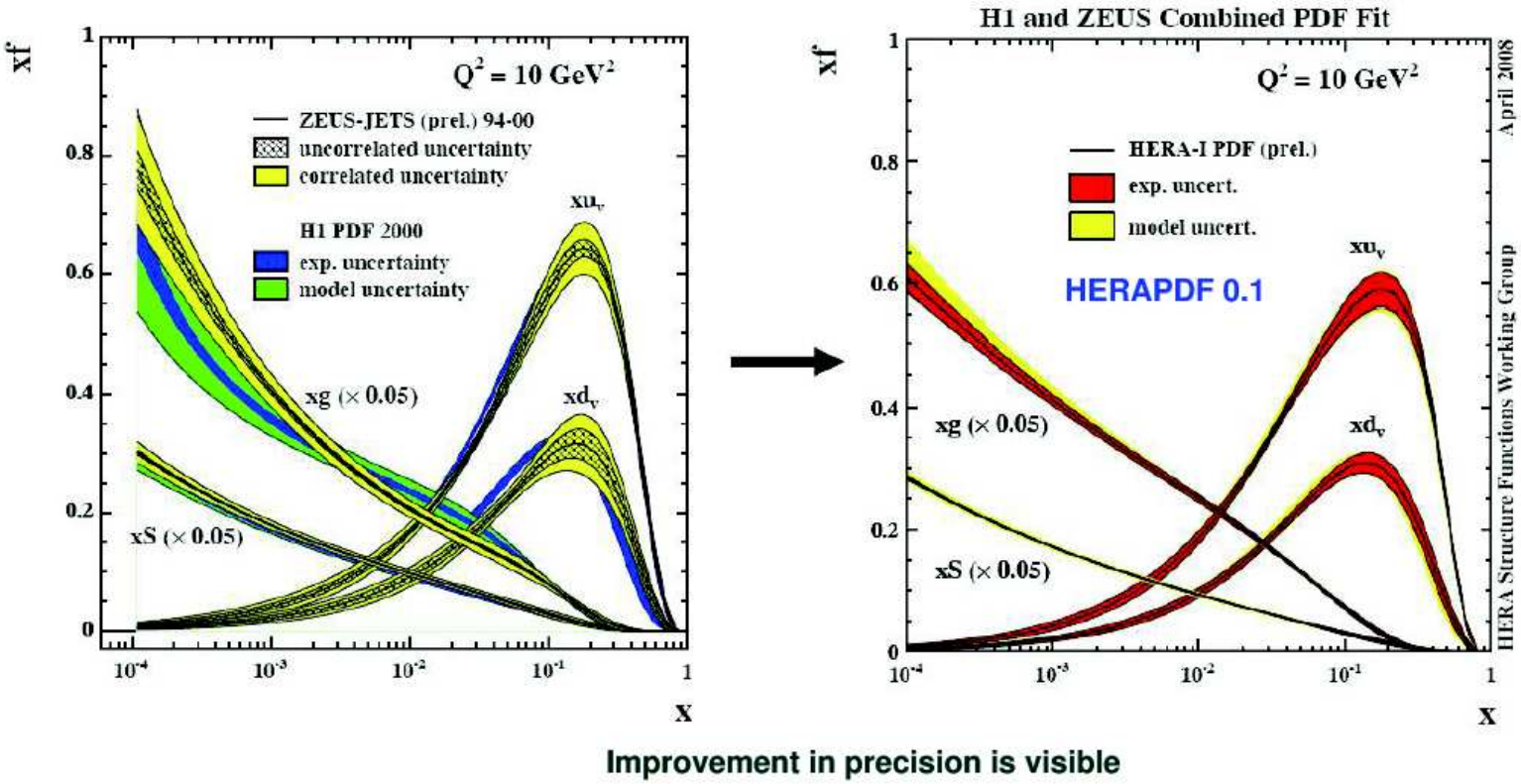

Improvement in precision is visible

Christinel Diaconu. HERA-LHC workshop, 2008

HERAPDF0.1 set based on the combined H1+ZEUS data

Smaller nominal PDF uncertainty as compared to CTEQ/MSTW; but

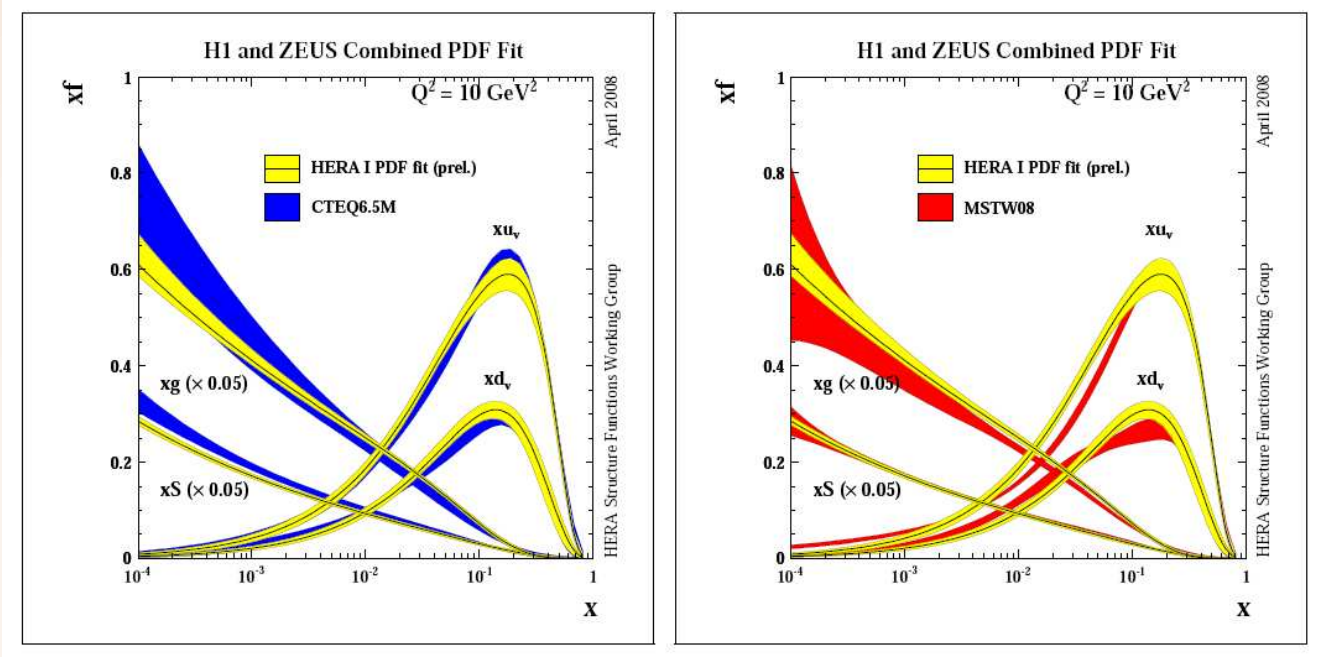

- insufficient PDF flavor separation (neutral-current DIS probes only $4/9\,(u+\bar{u}+c+\bar{c})+1/9\,(d+\bar{d}+s+\bar{s})$)
- more rigid PDF parametrizations (e.g., $g(x,Q_0)=Ax^B(1-x)^C$) $\Rightarrow$ less flexibility to probe the PDF behavior, notably at small x
- so far, a simplified (zero-mass scheme) treatment of charm and bottom mass dependence

Studies of tolerance in new approaches

Neural Network PDF collaboration

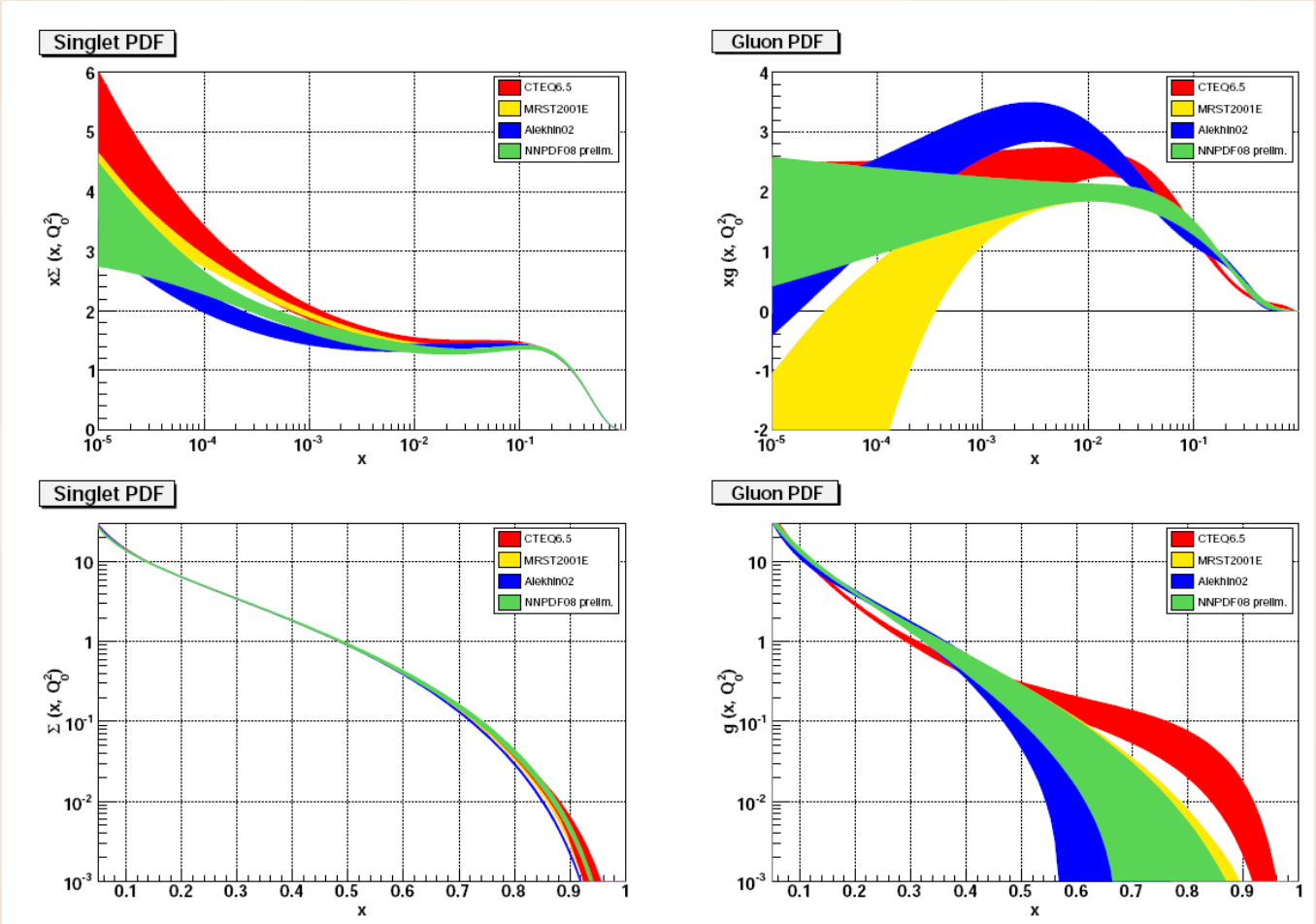

Biases due to the parametrization, Gaussian approximation for errors are reduced; better estimates for the PDF uncertainty may be feasible

Theoretical errors: uncertainties vs. mistakes

PDF error bands reflect *uncertainties* (a range of theoretical predictions for plausible input assumptions) due to

- experimental errors propagated into PDF's
- treatment of possible inconsistencies between experimental data sets
- dependence on factorization scales, choice of the PDF parametrization, treatment of higher twists, nuclear effects,...
- numerical approximations in PDF fits

The *uncertainties* must not be confused with *mistakes* caused by outdated assumptions in the previous analyses

Oversimplified treatment of heavy-quark (s, c, b) contributions is one such mistake that can no longer be tolerated

s, c, b: the least constrained sector of the nucleon structure

- Data from HERA, NuTeV, Tevatron is increasingly sensitive to heavier flavors
- Some theoretical constraints on $Q_{\pm}(x,\mu) = Q(x,\mu) \pm \bar{Q}(x,\mu)$ ($Q = s,\, c,\, b$) can be now released, and new PDF models can be examined
- opportunities for interesting QCD tests
  - QCD factorization with realistic $m_{c,b}$ dependence
  - studies of flavor asymmetries in the quark sea
- impact on BSM searches, general hadronic physics at the LHC, etc.

CTEQ6.5 and CTEQ6.6: advanced treatment of heavy quarks

1. full implementation of the **general-mass "SACOT-χ" scheme**

   - differences in predictions for c, b scattering ($F_2^{c,b}(x,Q^2)$, etc.), EW precision cross sections, as compared to the zero-mass CTEQ6.1

   Tung et al., JHEP 0702, 053 (2007); ***CTEQ6.5***

2. exploration of **free strange PDF's** and/or asymmetric strange sea

$$s_+(x) \neq r\left(\bar{u}(x)+\bar{d}(x)\right), \quad s_-(x) \neq 0,$$
$$\text{where } s_\pm(x) \equiv s(x) \pm \bar{s}(x)$$

   Lai et al., JHEP 0704, 089 (2007); ***CTEQ6.5S***

3. PDF's with **nonperturbative charm**

   - $c(x,\mu_0 = m_c) \neq 0$ due to low-energy charm excitations (as opposed to $g \to c\bar{c}$ radiative production)

   Pumplin et al., PRD 75, 054029 (2007); ***CTEQ6.5C***

CTEQ6.6 study consolidates these developments

PDF family	Number of PDF sets	$s_+(x)$	$s_-(x)$	$\alpha_s(M_Z)$	Nonpert. charm PDF
6.6	45	free	0	0.118	No

- CTEQ6.6M + **44** extreme eigenvector sets
  - $s_+(x)$ is **independent** of $\bar{u}(x) + \bar{d}(x)$
- $s_-(x) = 0$, in agreement with the data at 90% c.l.
  - the preference for $s_-(x) \neq 0$ remains marginal: $\Delta\chi^2 = -15$ for $\int_0^1 x s_-(x, \mu_0) dx = 0.0018$, $\sqrt{2N_{NuTeV}} = 22$

CTEQ6.6 study consolidates these developments

PDF family	Number of PDF sets	$s_+(x)$	$s_-(x)$	$\alpha_s(M_Z)$	Nonpert. charm PDF
6.6	45	free	0	0.118	No
6.6C	4	free	0	0.118	Yes

- CTEQ6.6C: updated PDF's with intrinsic charm

CTEQ6.6 study consolidates these developments

PDF family	Number of PDF sets	$s_+(x)$	$s_-(x)$	$\alpha_s(M_Z)$	Nonpert. charm PDF
6.6	45	free	0	0.118	No
6.6C	4	free	0	0.118	Yes
6.6A	4	free	0	0.112-0.125	No

- CTEQ6.6C: updated PDF's with intrinsic charm
- CTEQ6.6A: PDF's for $\alpha_s(M_Z) = 0.112 - 0.125$

CTEQ6.6 study consolidates these developments

PDF family	Number of PDF sets	$s_+(x)$	$s_-(x)$	$\alpha_s(M_Z)$	Nonpert. charm PDF
6.6	45	free	0	0.118	No
6.6C	4	free	0	0.118	Yes
6.6A	4	free	0	0.112-0.125	No

- CTEQ6.6C: updated PDF's with intrinsic charm
- CTEQ6.6A: PDF's for $\alpha_s(M_Z) = 0.112 - 0.125$
- All CTEQ6.6 sets are provided for $10^{-8} \leq x \leq 1$

CTEQ6.6 PDF's

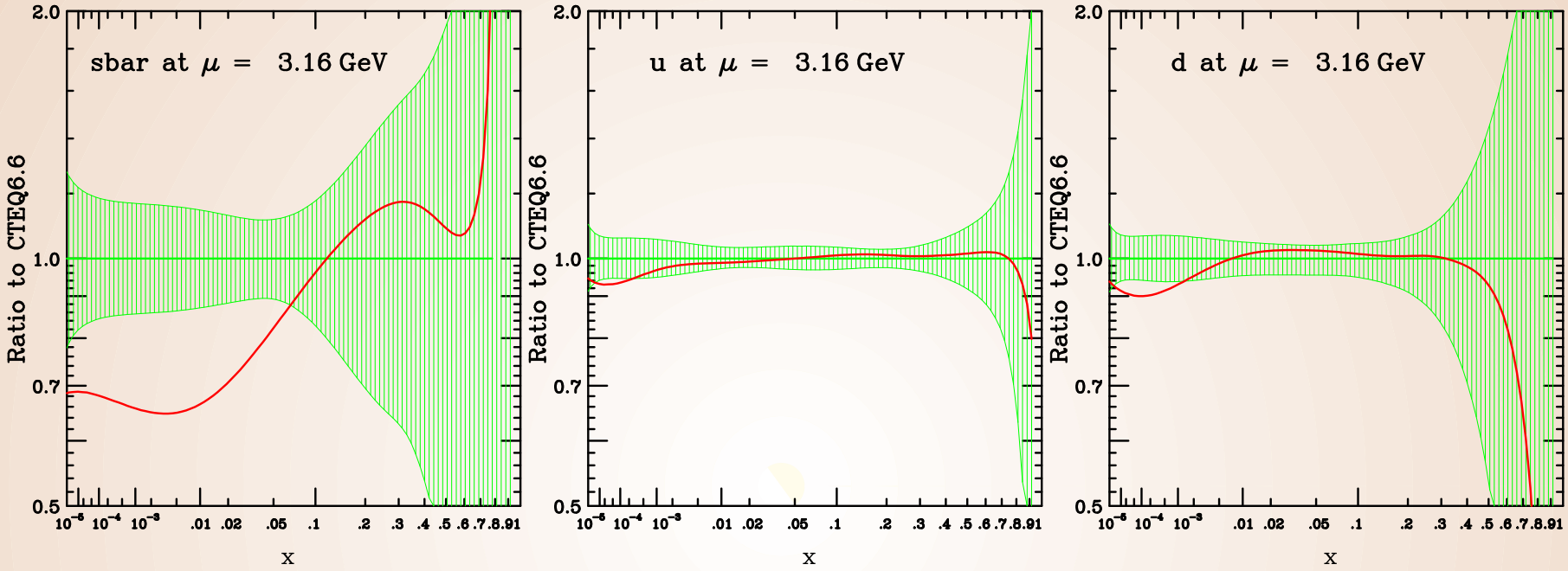

dashes: CTEQ6.1M (zero-mass scheme)

- very different strange PDF's
- CTEQ6.6 u, d are above CTEQ6.1 at $x \lesssim 10^{-2}$
  - The result of suppressed charm contribution to $F_2(x, Q)$ at HERA in the GM-VFN scheme

General-mass (ACOT-χ) factorization scheme

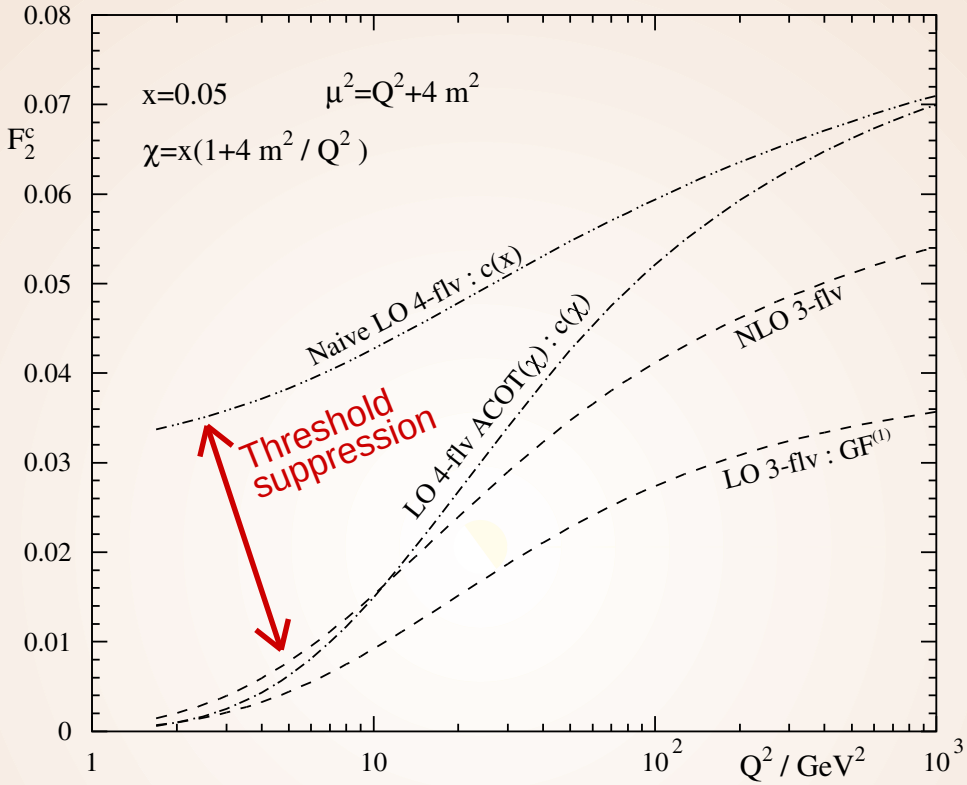

- Charm Wilson coefficient function is suppressed at $Q \to m_c$
- To keep agreement with DIS F_2 data, u, d, $\bar{u}$, $\bar{d}$ PDF's are enhanced at small x, as compared to the zero-mass (ZM-VFN) scheme

Z and W production as "standard candle" processes

- Event rates for $pp \to W^{\pm}X$, $pp \to Z^0 X$ at the LHC can be measured with accuracy $\delta\sigma/\sigma \sim 1\%$ (tens of millions of events even at low luminosity)
- These measurements will be employed to tightly constrain PDF's and monitor the LHC luminosity $\mathcal{L}$ in real time

  (Dittmar, Pauss, Zurcher; Khoze, Martin, Orava, Ryskin; Giele, Keller';...)

  - other methods will initially give $\delta\mathcal{L} = 10 - 20\%$
- Various cross section measurements will be normalized to Z, W cross sections

W and Z rapidity distributions at NNLO

(Anastasiou, Dixon, Melnikov, Petriello, 2003)

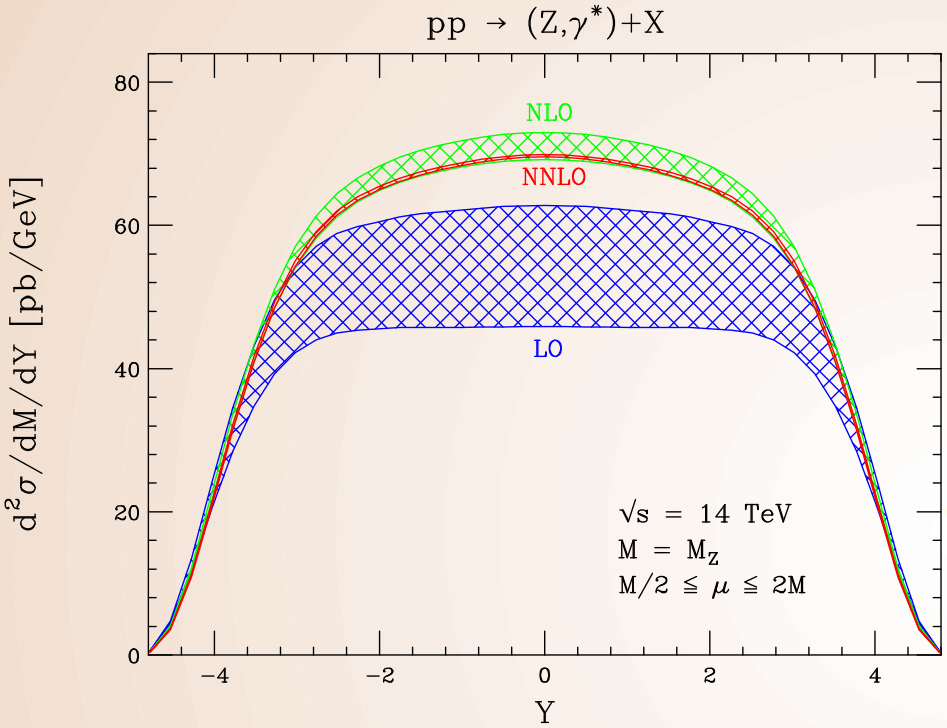

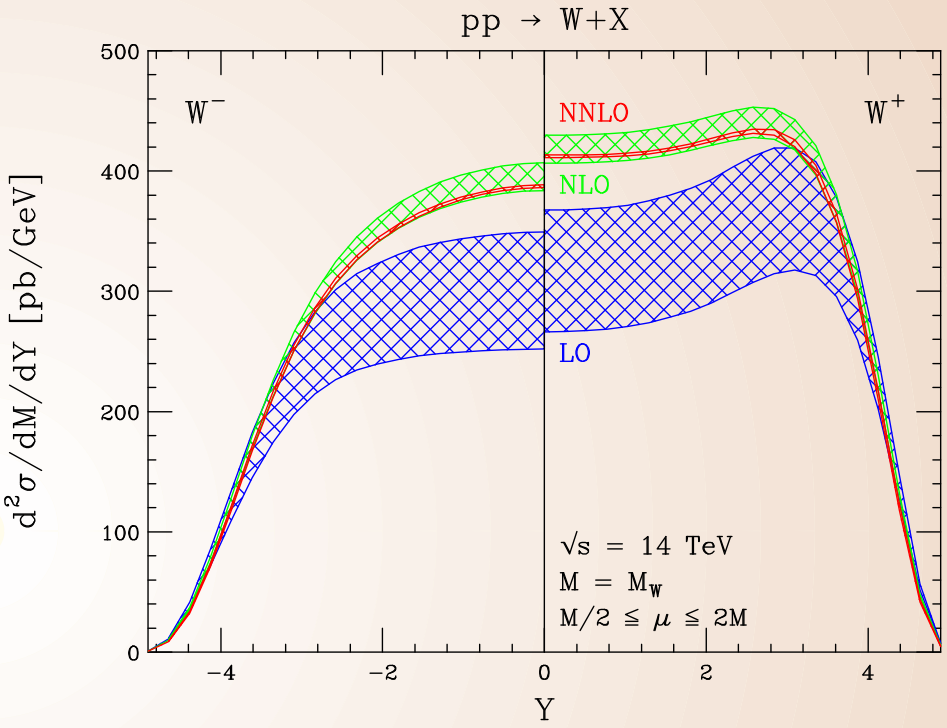

- Tiny scale dependence ($\sim 1\%$)
- For $|y| < 2$, NNLO leads to a uniform rescaling

$$\sigma_{NNLO} \approx K_{NNLO} \cdot \sigma_{NLO};\ K^{LHC}_{NNLO} \approx 0.98$$

- Larger corrections at forward rapidities

CTEQ6.6 W and Z cross sections at the LHC

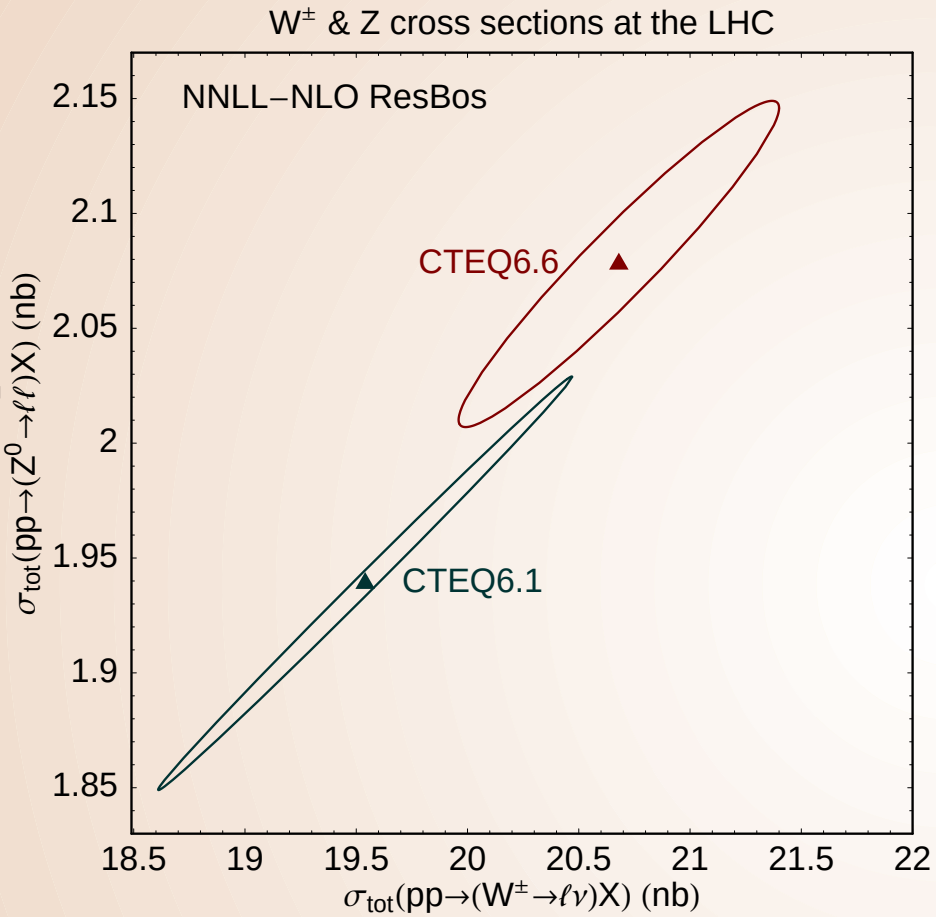

- Computation done with NNLL-NLO ResBos *(Balazs, Ladinsky, P.N., Yuan)*, with the goal to estimate *relative* differences due to NLO/NNLO PDFs
- Effect of NNLO hard + NLO EW contributions is nearly independent of PDF's
- Ellipses: the PDF uncertainty for $\Delta\chi^2_{scaled} = 100$ (<90% c.l. for 2-dim dependence)

General-mass CTEQ6.6 predictions are higher by 6-7% compared to zero-mass CTEQ6.1 (enhanced CTEQ6.6 u, d PDF's at $x \sim 0.005$)

W and Z cross sections at the LHC

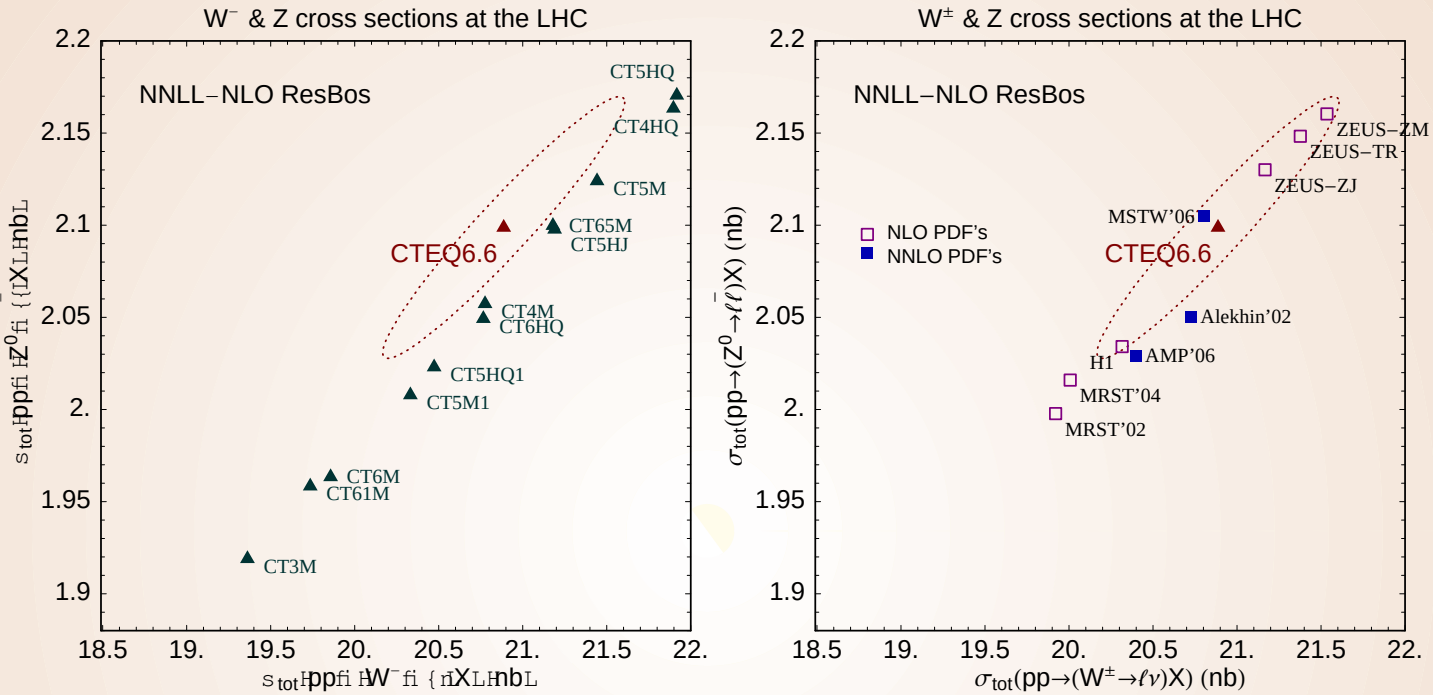

- Such changes in $\sigma_{Z,W}$ exceed NNLO corrections of $\approx -2\%$ or anticipated experimental error of $\sim 1\%$
- MSTW 2006 and 2008 predictions became compatible with the CTEQ6.6 result

PDF-induced correlations in W, Z, $t\bar{t}$ production

$W - Z$: correlated dependence

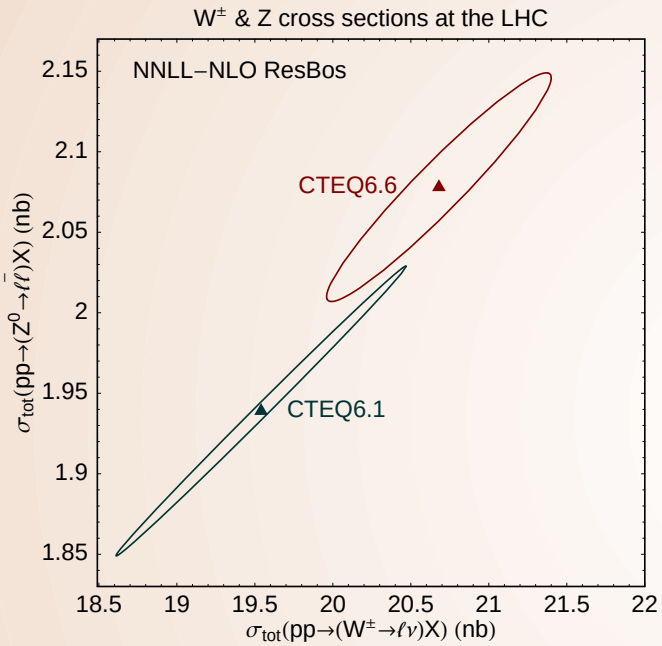

$W - t\bar{t}$ (or $Z - t\bar{t}$): anti-correlated dependence

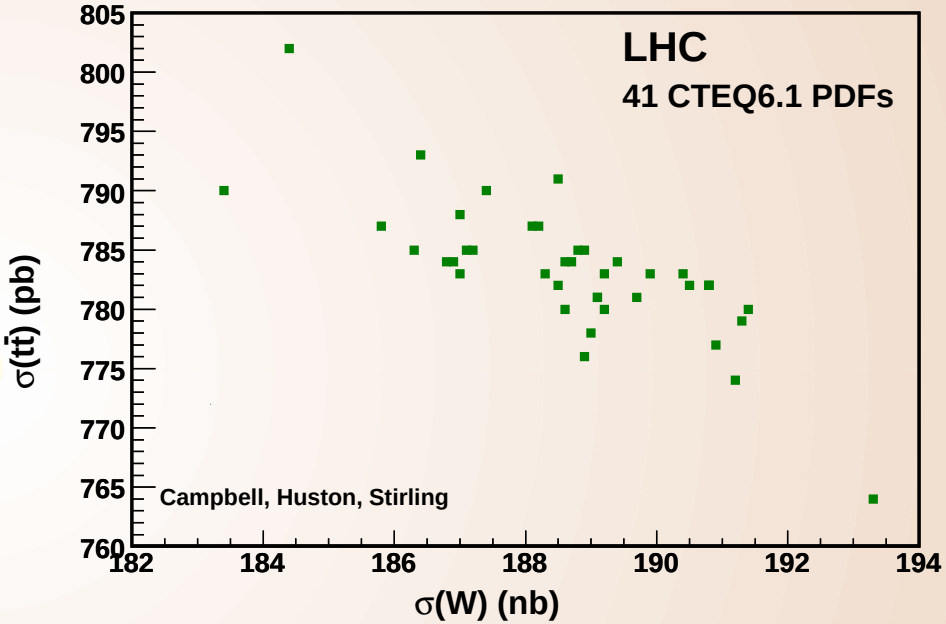

- Which parton flavors drive the "experimental" PDF uncertainties and lead to (anti-)correlations between the cross sections?
- The PDF dependence of a cross section ratio σ_1/σ_2 is reduced (enhanced) if σ_1 and σ_2 are correlated (anticorrelated)

PDF-induced correlations in W, Z, $t\bar{t}$ production

$W - Z$: correlated dependence

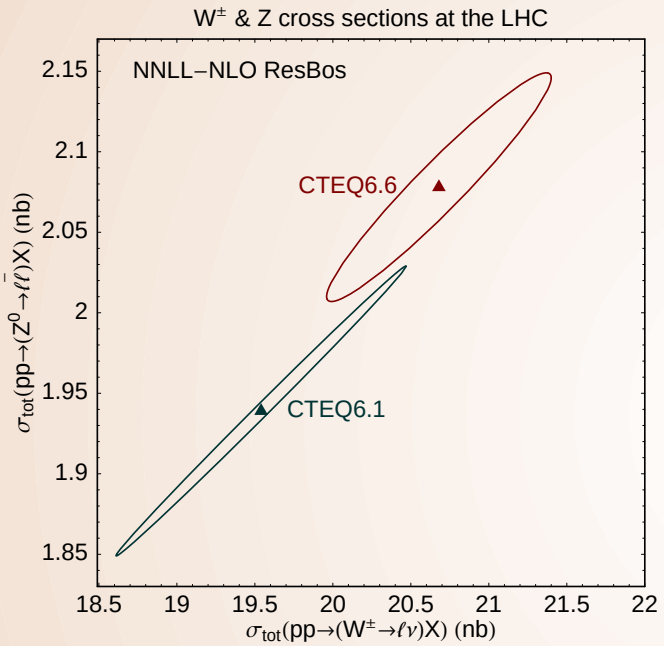

$W - t\bar{t}$ (or $Z - t\bar{t}$): anti-correlated dependence

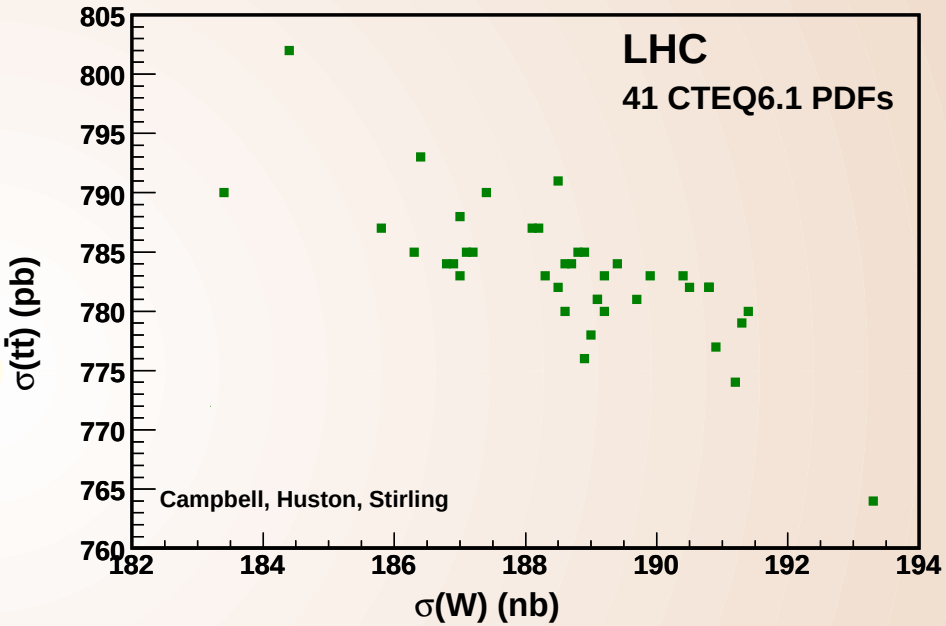

- How can we reduce the remaining PDF uncertainties?
- Ideally, we would like to relate $\delta_{PDF}\sigma$ to (a few) specific $f_a(x, \mu)$

Experimental PDF errors: which measurements can reduce them?

Knowing what to measure and how to measure it makes a complicated world much less so.

The conventional wisdom is often wrong.

S. D. Levitt, S. J. Dubner, Freakonomics

PDF dependence of collider processes

- Correlation analysis can be applied to understand rich PDF-induced relations between physical observables
- Naive views about the PDF dependence tend to be misleading

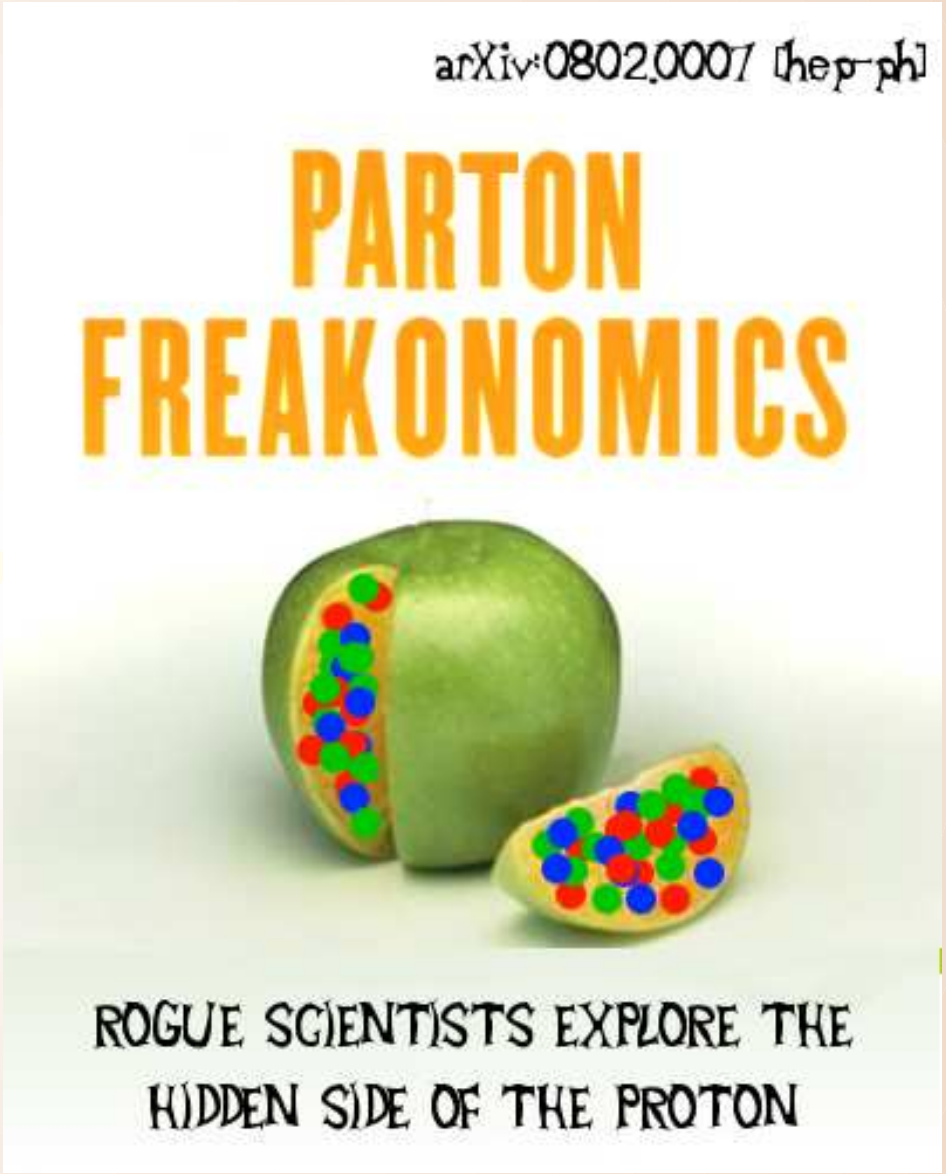

Z production at the LHC

Choose all that apply and select the x range

The PDF uncertainty in σ_Z is mostly due to...

1. u, d, $\bar{u}$, $\bar{d}$ PDF's
   at $x < 10^{-2}$ ($x > 10^{-2}$)
2. gluon PDF
   at $x < 10^{-2}$ ($x > 10^{-2}$)
3. s, c, b PDF's
   at $x < 10^{-2}$ ($x > 10^{-2}$)

Leading order

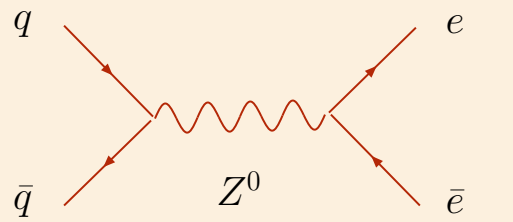

Next-to-leading order

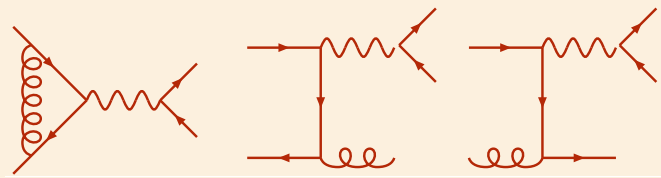

An inefficient application of the error analysis

☺ Compute σ_Z for 40 (now 44) extreme PDF eigensets

☺ Find eigenparameter(s) producing largest variation(s), such as #9, 10, 30

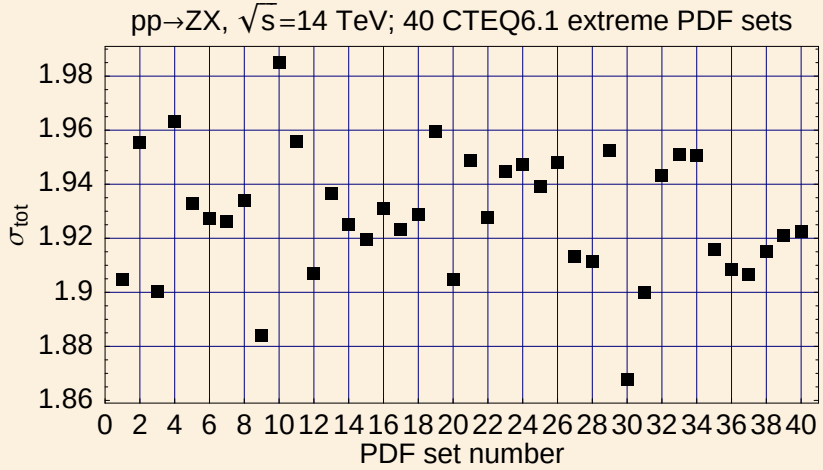

☹ It is not obvious how to relate abstract eigenparameters to physical PDF's $u(x)$, $d(x)$, etc.

Correlation analysis for collider observables

(J. Pumplin et al., PRD 65, 014013 (2002); P.N. and Z. Sullivan, hep-ph/0110378)

A technique based on the Hessian method to relate the PDF uncertainty in physical cross sections to PDF's of specific flavors at known (x, μ)

For $2N$ PDF eigensets and two cross sections X and Y:

$$\Delta X = \frac{1}{2}\sqrt{\sum_{i=1}^{N}\left(X_i^{(+)} - X_i^{(-)}\right)^2}$$

$$\cos\varphi = \frac{1}{4\Delta X\,\Delta Y}\sum_{i=1}^{N}\left(X_i^{(+)} - X_i^{(-)}\right)\left(Y_i^{(+)} - Y_i^{(-)}\right)$$

$X_i^{(\pm)}$ are maximal (minimal) values of X_i tolerated along the i-th PDF eigenvector direction; $N = 22$ for the CTEQ6.6 set

Correlation angle φ

Determines the parametric form of the $X - Y$ correlation ellipse

$$X = X_0 + \Delta X \cos\theta$$
$$Y = Y_0 + \Delta Y \cos(\theta + \varphi)$$

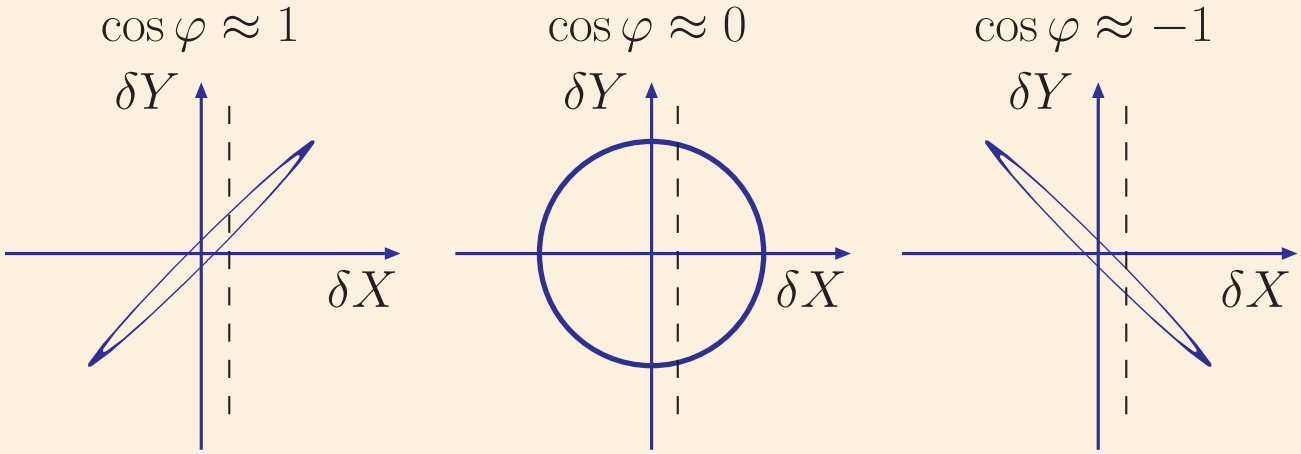

X_0, Y_0: best-fit values

ΔX, ΔY: PDF errors

$\cos\varphi \approx \pm 1$: Measurement of X imposes tight constraints on Y

$\cos\varphi \approx 0$: Measurement of X imposes loose constraints on Y

Types of correlations

X and Y can be

- two PDFs $f_1(x_1, Q_1)$ and $f_2(x_2, Q_2)$ (plotted as $\cos\varphi$ vs x_1 & x_2)
- a physical cross section σ and PDF $f(x, Q)$ (plotted as $\cos\varphi$ vs x)
- two cross sections σ_1 and σ_2

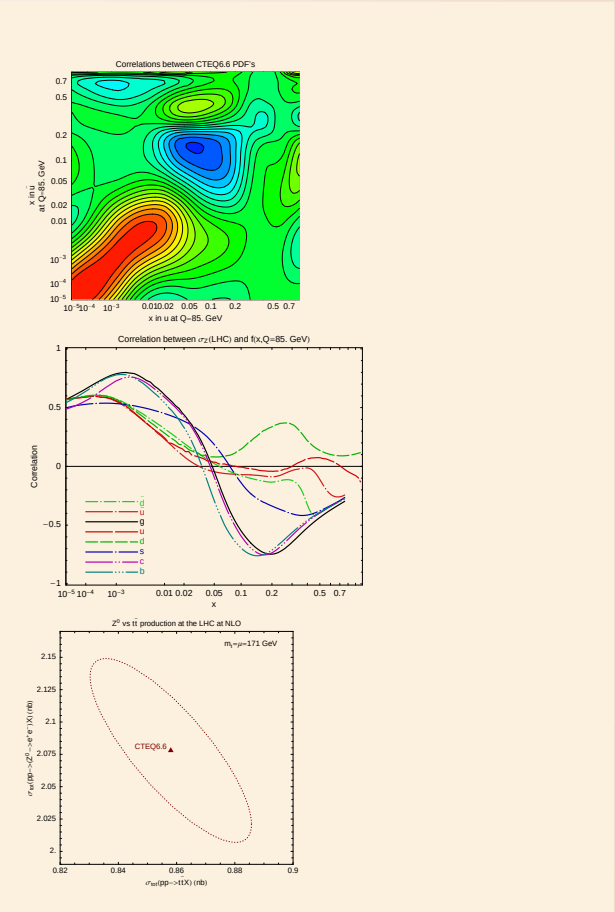

Correlations $\cos\varphi$ between W, Z cross sections and PDF's

Tevatron Run-2

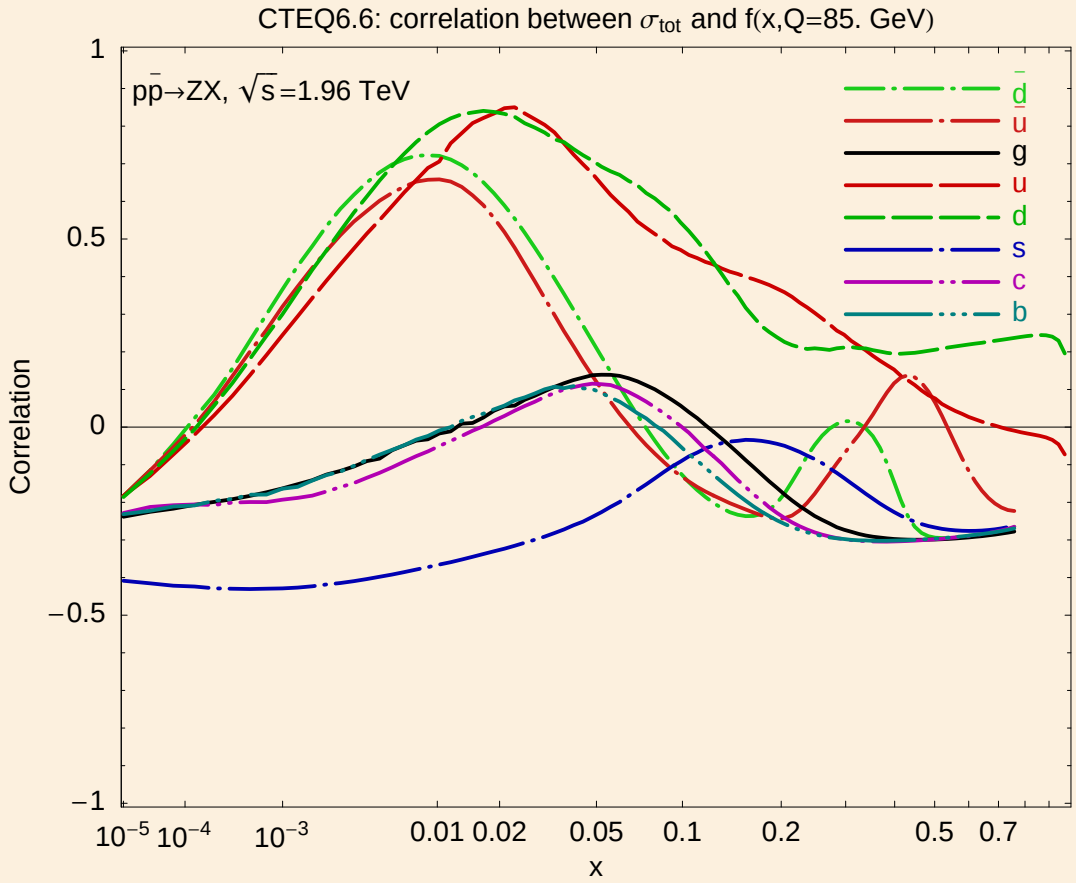

Similar correlations for W production

Correlations $\cos\varphi$ between W, Z cross sections and PDF's

LHC

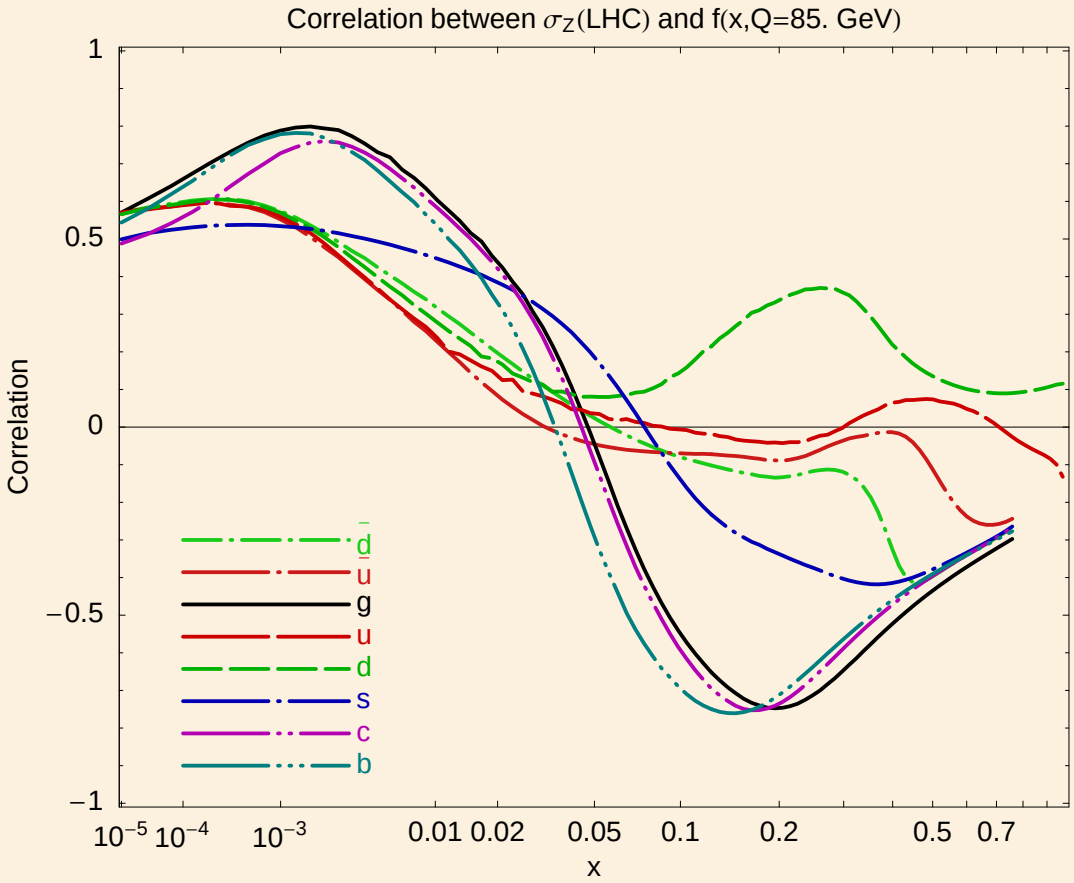

Tevatron Run-2

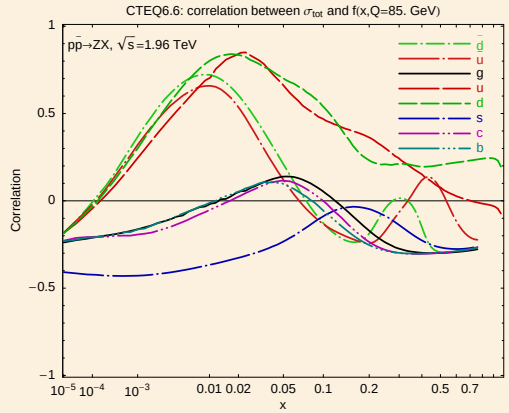

Similar correlations for W production

Correlations of Z and $t\bar{t}$ cross sections with PDF's

LHC Z, W cross sections are strongly correlated with $g(x)$, $c(x)$, $b(x)$ at $x \sim 0.005$

$\therefore$ they are strongly anticorrelated with processes sensitive to $g(x)$ at $x \sim 0.1$
($t\bar{t}$, $gg \to H$ for $M_H > 300$ GeV)

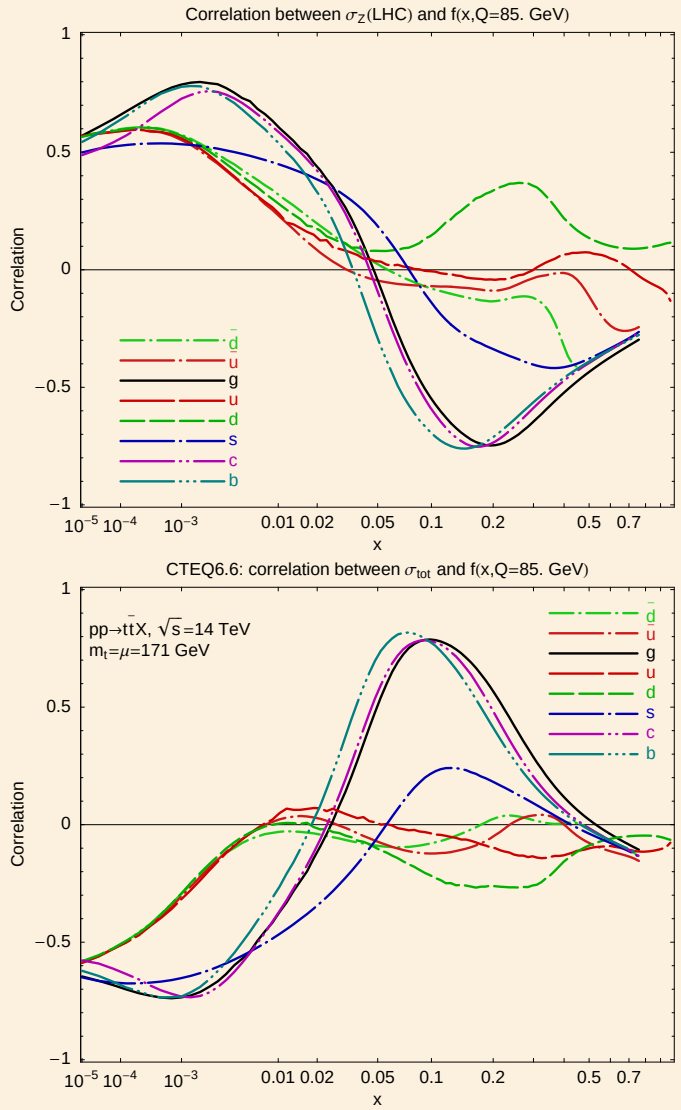

$t\bar{t}$ vs Z cross sections at the LHC

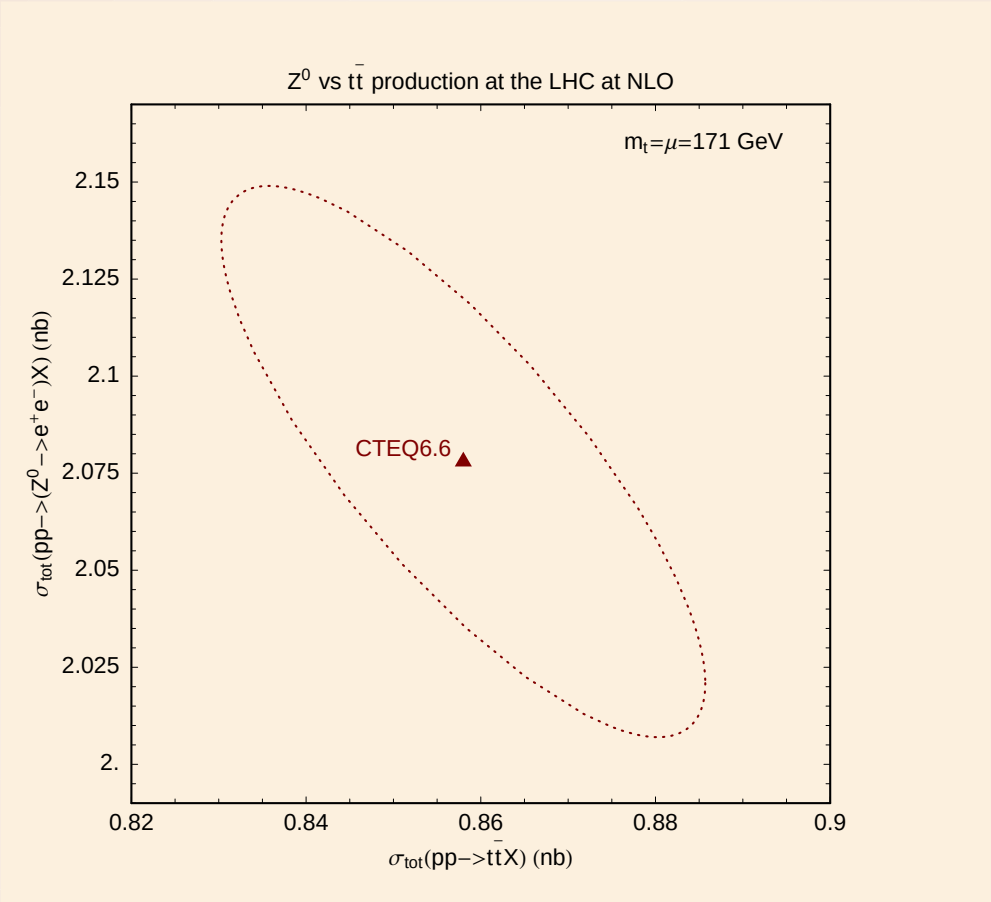

Measurements of $\sigma_{t\bar{t}}$ and σ_Z probe the same (gluon) PDF degrees of freedom at different x values

Correlations between $\sigma(gg \to H^0)$, σ_Z, $\sigma_{t\bar{t}}$

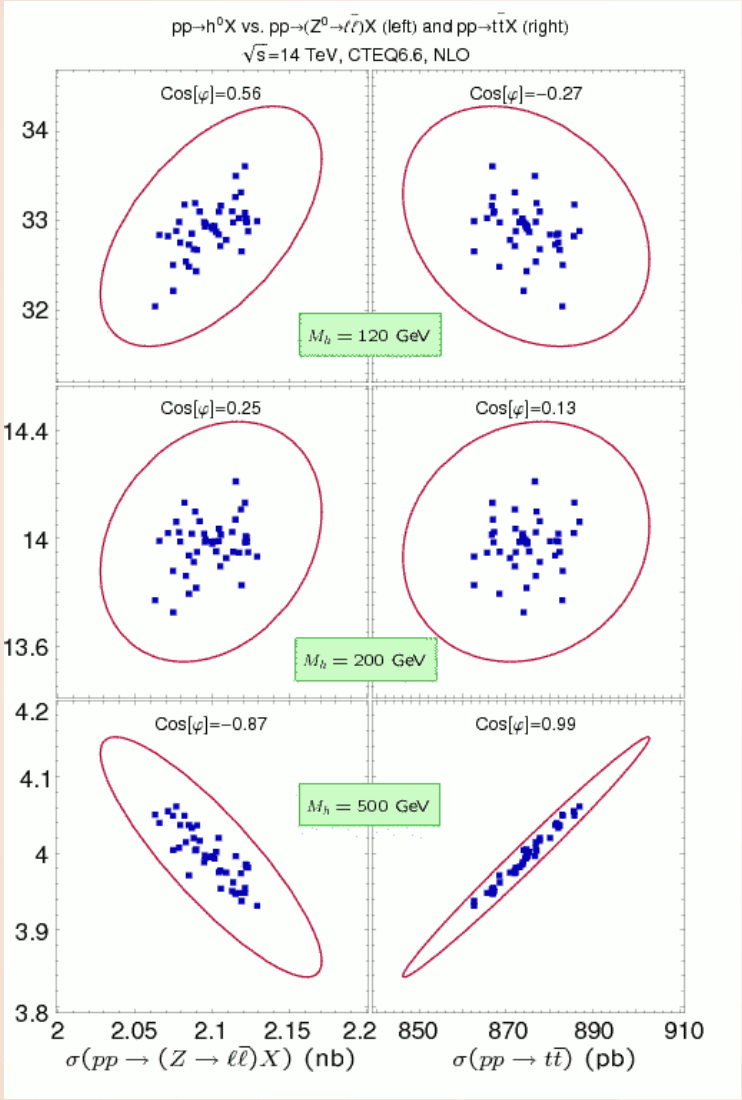

As M_H increases:

- $\cos\varphi(\sigma_H, \sigma_Z)$ decreases
- $\cos\varphi(\sigma_H, \sigma_{t\bar{t}})$ increases

$\cos\varphi$ for various NLO Higgs production cross sections in SM and MSSM

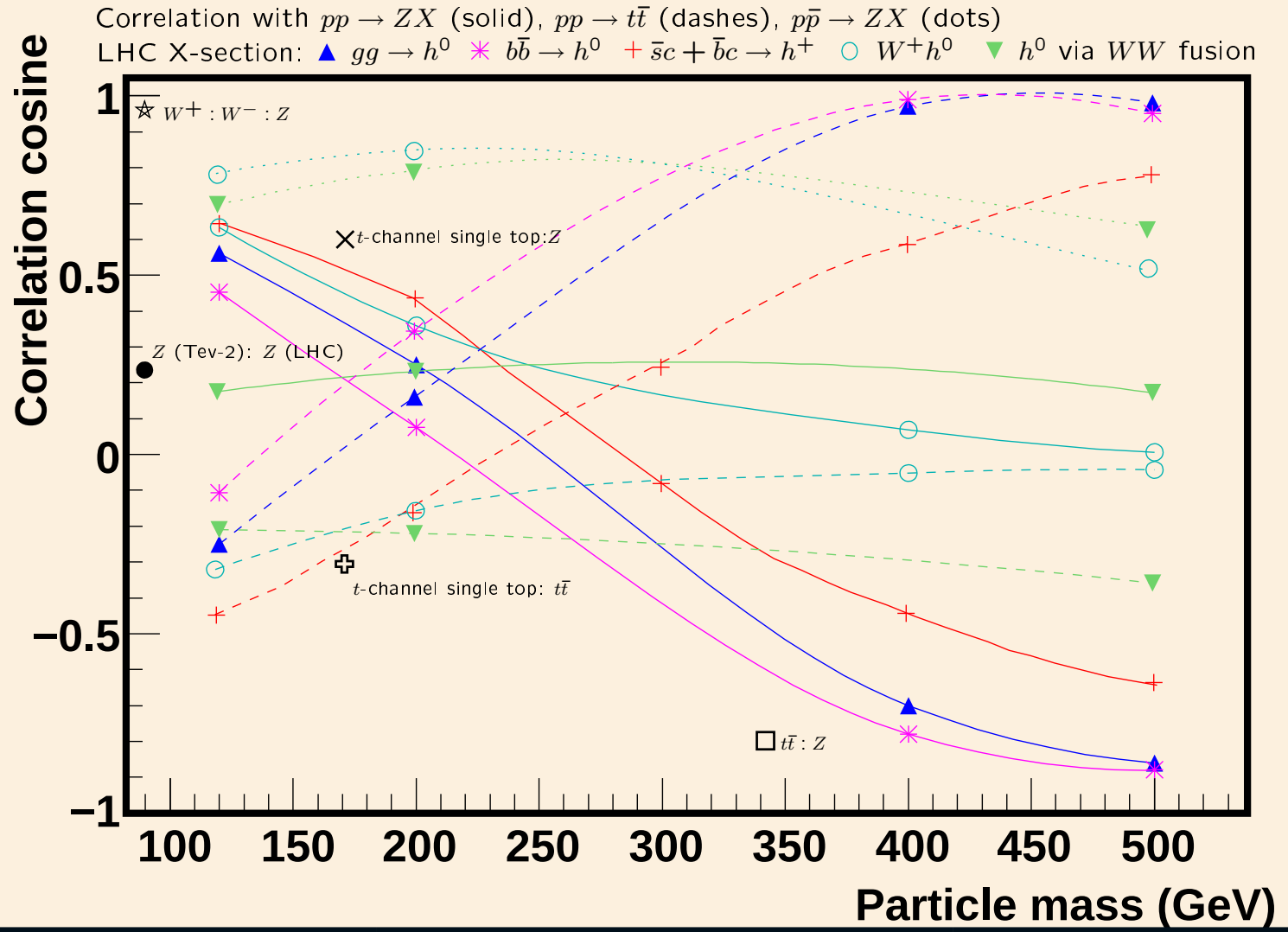

An example of a small correlation with the gluon

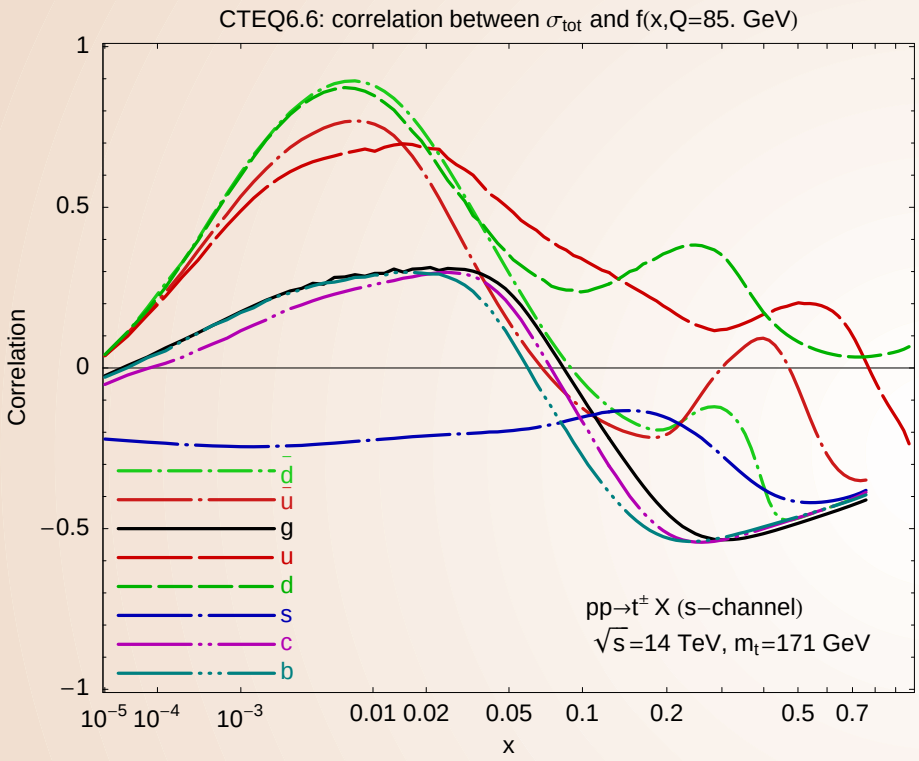

Single-top production (NLO)

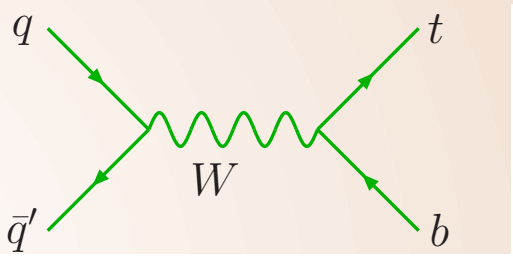

- typical $x \sim 0.01$
- mostly correlated with u, d PDF's

PDF uncertainties in W, Z *total* cross sections are irrelevant for some quark scattering processes (single-top, Z', ...)

W and Z cross sections and their ratio

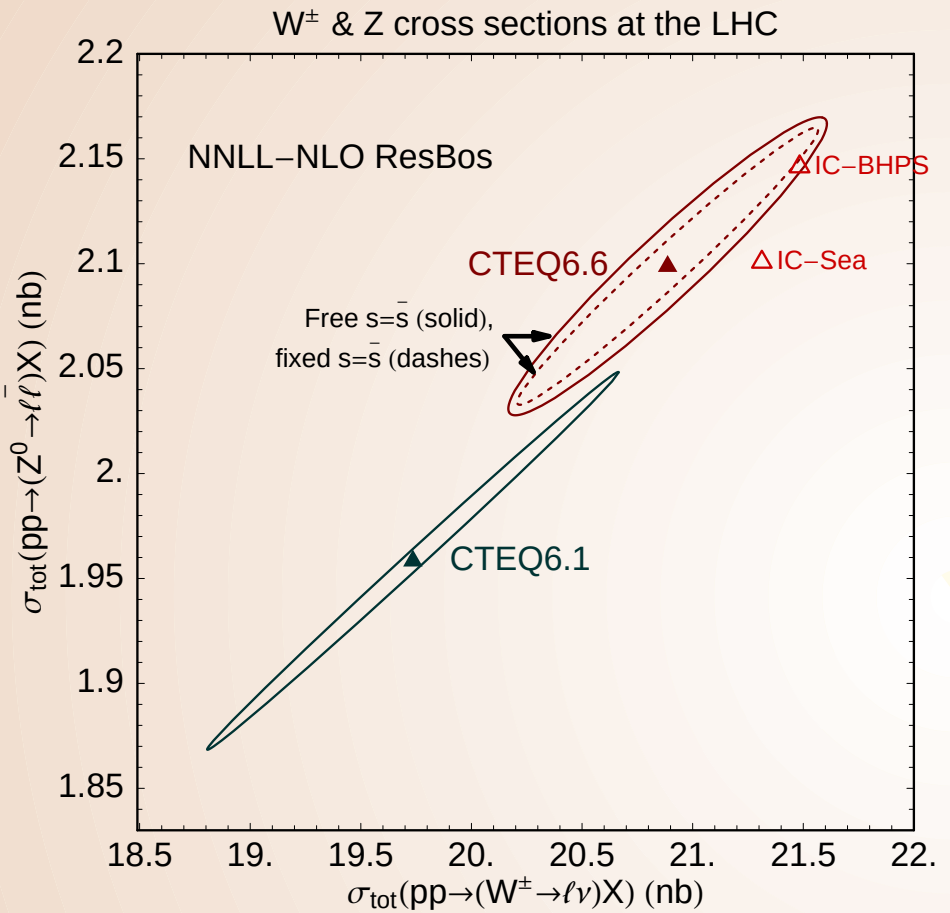

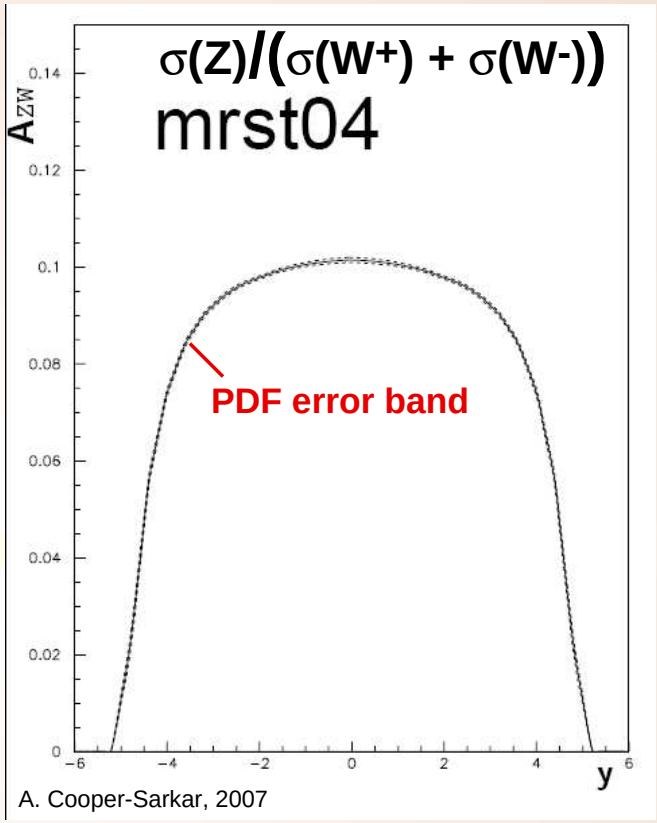

- Radiative contributions have similar structure in $W^{\pm}$ and Z cross sections; cancel well in Xsection ratios
- The PDF uncertainty cancels partially because of differences in s, c, b scattering contributions

W and Z cross sections and their ratio

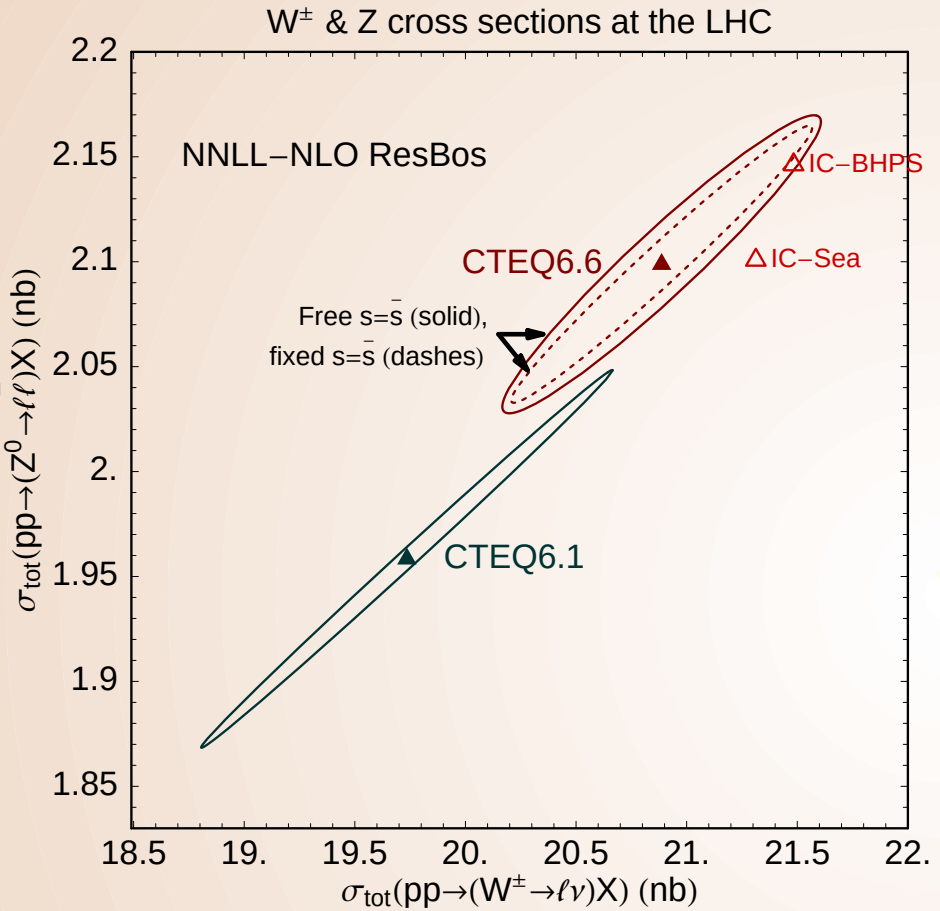

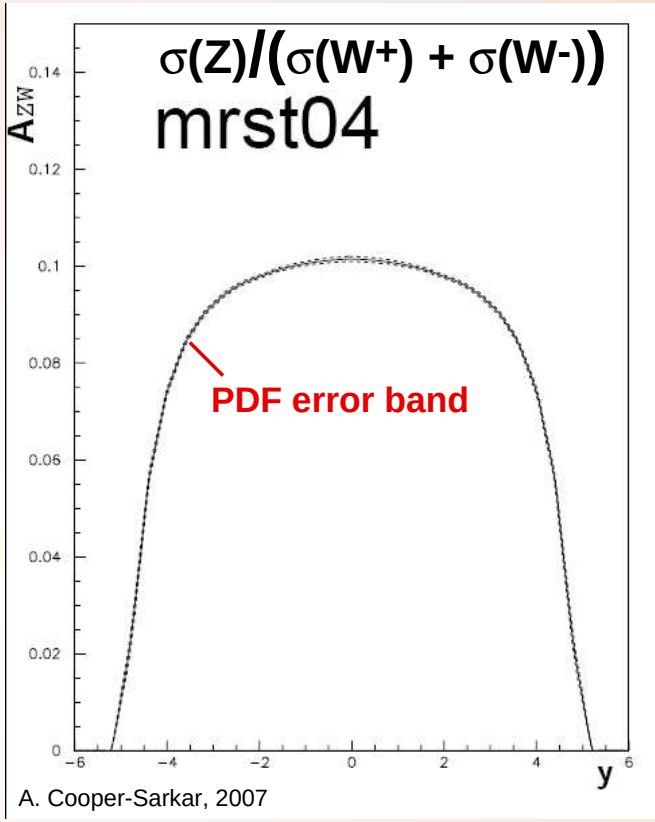

- 27% of $\sigma_{NLO}(W^{\pm})$ from $c\bar{s} \to W^{\pm}$, 20% of $\sigma_{NLO}(Z^0)$ from $s\bar{s} \to Z^0$
- non-negligible effects from free strangeness and intrinsic charm (IC) PDF's

σ_Z/σ_W at the LHC

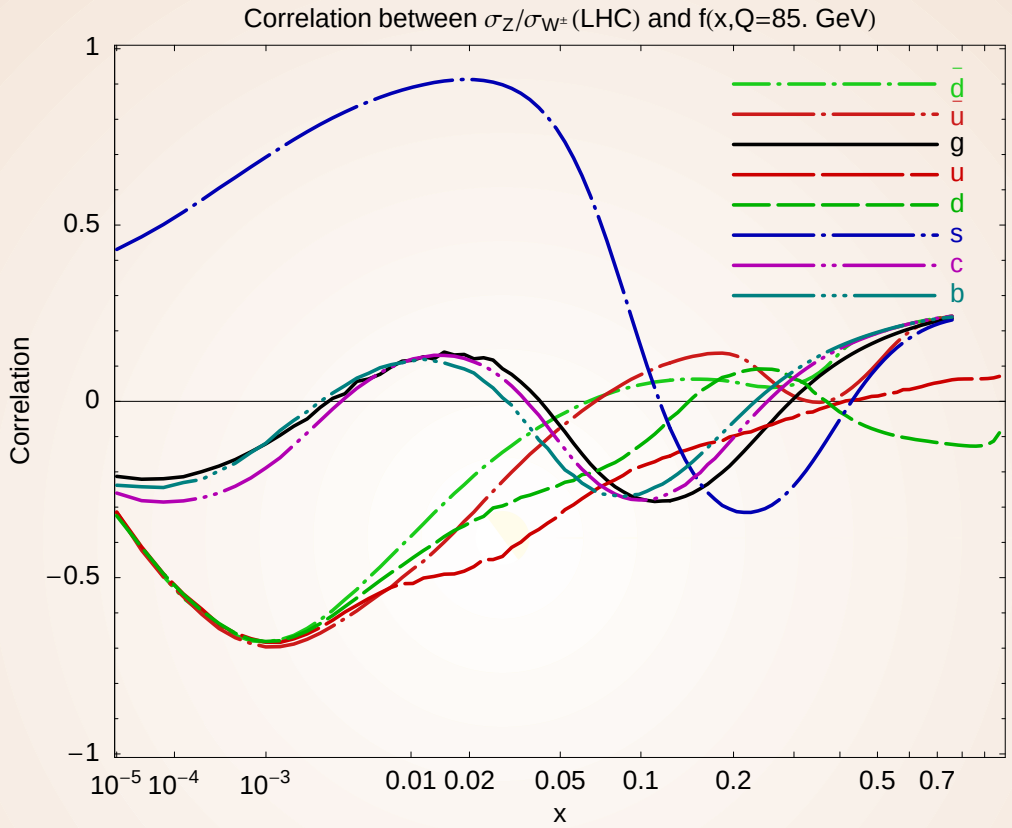

The remaining PDF uncertainty in σ_Z/σ_W is mostly driven by $s(x)$; increases by a factor of 3 compared to CTEQ6.1 as a result of free strangeness in CTEQ6.6

Special PDF's with nonperturbative charm

(Pumplin et al., 2007; updated in CTEQ6.6C)

Three models responsible for intrinsic charm generation (light-cone, meson-cloud, and phenomenological sea-like), with $\langle x \rangle_{c+\bar{c}}$ up to 3.5% at scale Q_0

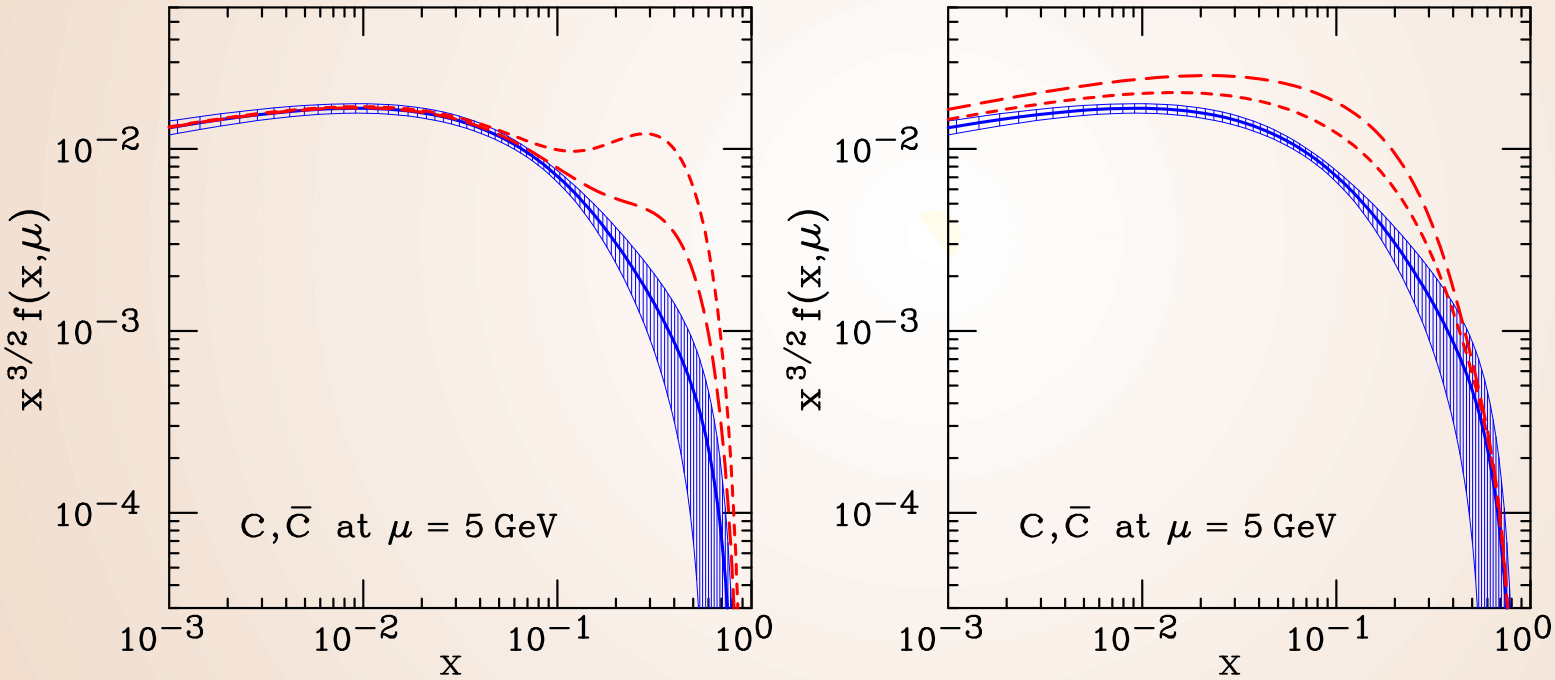

The enhancement in $c(x, Q)$ persists at all practical Q, can be observed at the Tevatron and LHC

$c\bar{s} + c\bar{b} \to H^+$ in 2-Higgs doublet model at the LHC

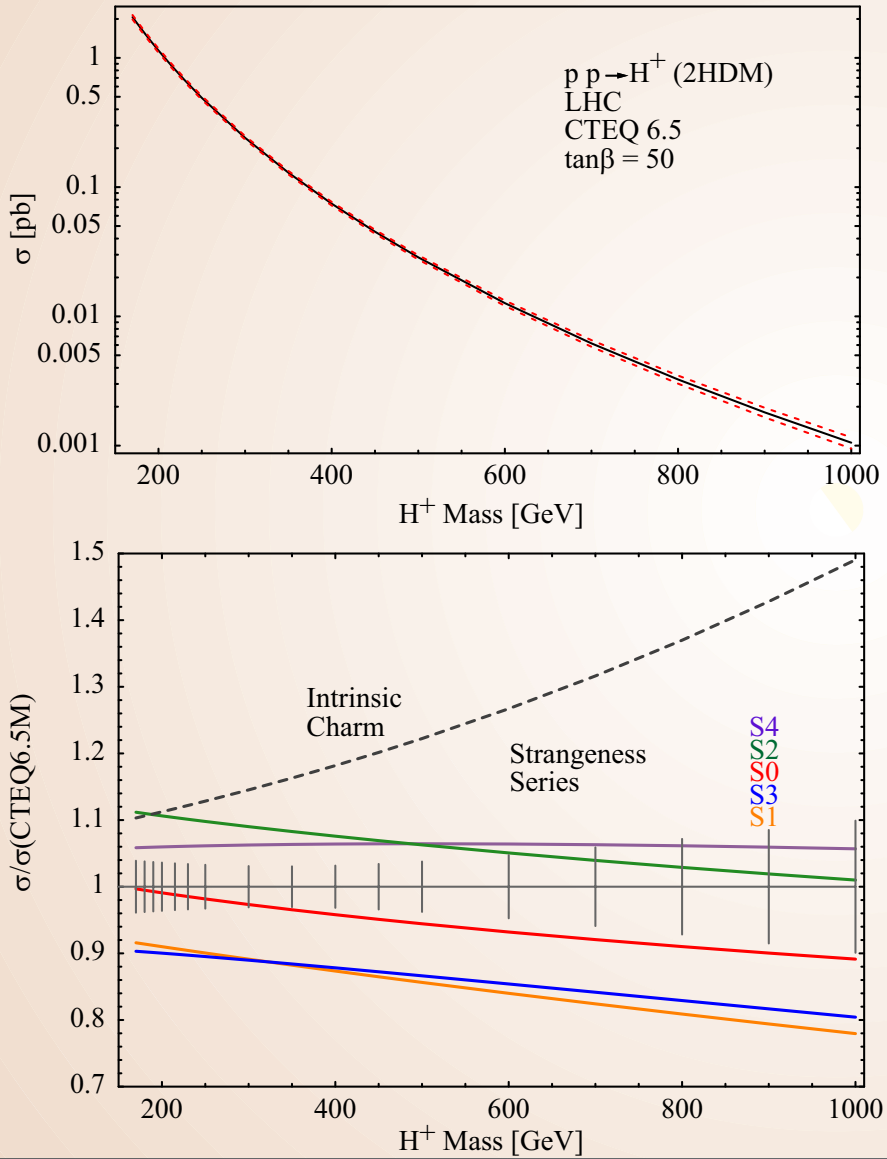

CTEQ6.6M uncertainty band covers most of the CTEQ6.5 uncertainty due to strangeness

"Maximum-strength" sea-like IC leads to large enhancement $\Rightarrow$ new measurements ($p\bar{p} \to ZcX$?) are needed to constrain it!

Conclusions

- Narrow PDF error bands can be misleading; theoretical improvements for all fitted experiments and the analysis of the entirety of contributing factors must continue
- CTEQ6.6 PDF's in the general-mass scheme:
  - important differences from ZM-VFNS and some CTEQ6.5 predictions
  - must be used as the standard CTEQ set from now on
- A new technique to study PDF-induced correlations between physical observables
- other ongoing efforts: NNLO/small-x/Q_T resummation in the global fits, impact of Run-2 jet data on the gluon PDF, PDF's for leading-order Monte-Carlos, a ROOT interface for PDF reweighting in Monte-Carlo programs; stay tuned!

Backup slides

General-mass variable-flavor number scheme

(Aivasis et al.; Chuvakin et al.; Thorne, Roberts; Kniehl et al.; Buza et al.; Cacciari et al.; ...)

- A series of effective fixed-flavor number (FFN) schemes, with N_f (the number of active parton flavors) incremented sequentially at momentum scales $\mu_{N_f} \approx m_{N_f}$
- incorporates essential $m_{c,b}$ dependence near, and away from, heavy-flavor thresholds

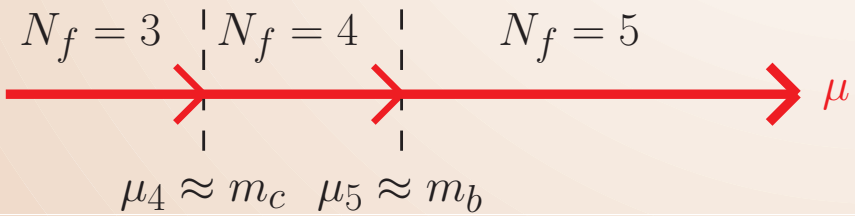

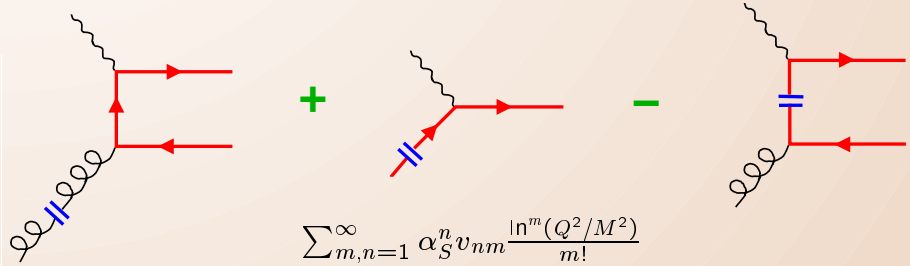

General-mass variable-flavor number scheme

(Aivasis et al.; Chuvakin et al.; Thorne, Roberts; Kniehl et al.; Buza et al.; Cacciari et al.; ...)

Proved for *inclusive DIS* by J. Collins (1998)

$$F_2(x,Q,m_c) = \sum_a \int_\chi^1 \frac{d\xi}{\xi} H_a(\frac{\chi}{\xi}, \frac{Q}{\mu}, \frac{m_c}{Q}) f_a(\xi, \frac{\mu}{m_c}) + \mathcal{O}\left(\frac{\Lambda_{QCD}}{Q}\right)$$

- $\lim_{Q\to\infty} H$ exists and is infrared safe
- collinear logarithms $\sum_{k,n=1}^{\infty} \alpha_s^k v_{kn} \ln^n(\mu/m_c)$ are resummed in $f_c(x,\mu/m_c)$
- no terms $\mathcal{O}(m_c/Q)$ in the remainder

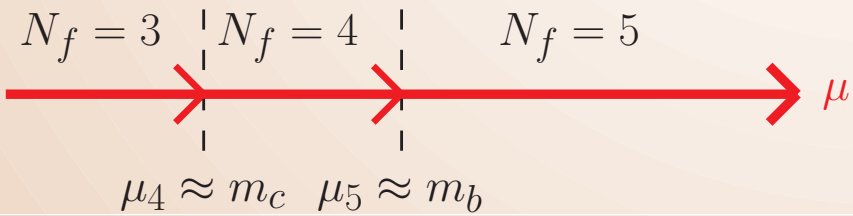

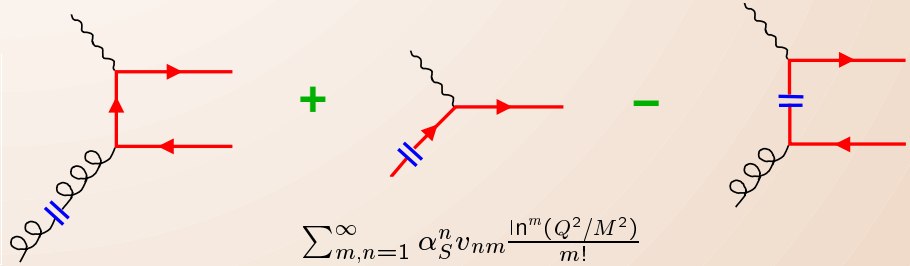

General-mass variable-flavor number scheme

(Aivasis et al.; Chuvakin et al.; Thorne, Roberts; Kniehl et al.; Buza et al.; Cacciari et al.; ...)

Proved for *inclusive DIS* by J. Collins (1998)

$$F_2(x,Q,m_c) = \sum_a \int_\chi^1 \frac{d\xi}{\xi} H_a(\frac{\chi}{\xi}, \frac{Q}{\mu}, \frac{m_c}{Q}) f_a(\xi, \frac{\mu}{m_c}) + \mathcal{O}\left(\frac{\Lambda_{QCD}}{Q}\right)$$

- Works most effectively in DIS and Drell-Yan-like processes; practical implementation requires
  1. efficient treatment of mass dependence, rescaling of momentum fractions χ in processes with incoming c, b
  2. physically motivated factorization scale to ensure fast PQCD convergence (e.g., $\mu = Q$ in DIS)

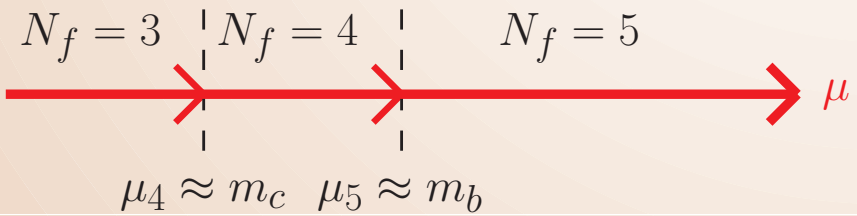

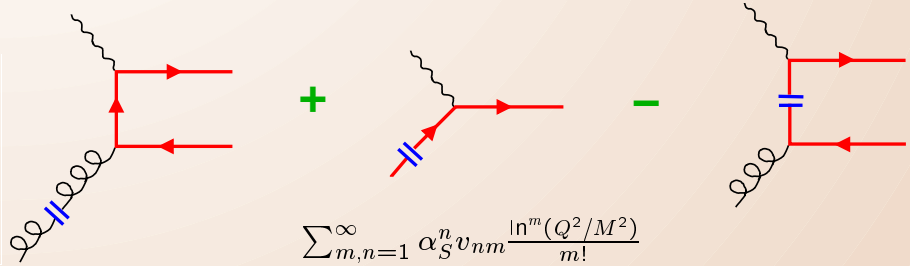

Simplified ACOT (χ) factorization scheme

- Defined with $m_c = 0$ in Wilson coefficient functions H with *incoming* charm quarks *(Collins; Kramer, Olness, Soper)*
  - simplifications! close to the full ACOT scheme numerically
- Rescaled momentum fractions χ *(Barnett, Haber, Soper; Tung, Kretzer, Schmidt)*

In neutral-current DIS: $\chi = \begin{cases} x & \text{for incoming } g, q \\ x\left(1 + \frac{4m_c^2}{Q^2}\right) & \text{for incoming } c \end{cases}$

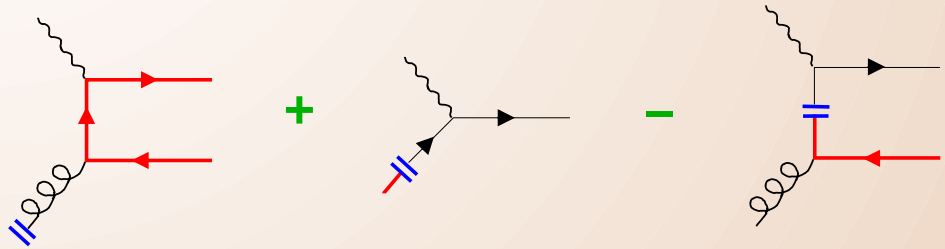

Tolerance hypersphere in the PDF space

2-dim (i,j) rendition of N-dim (22) PDF parameter space

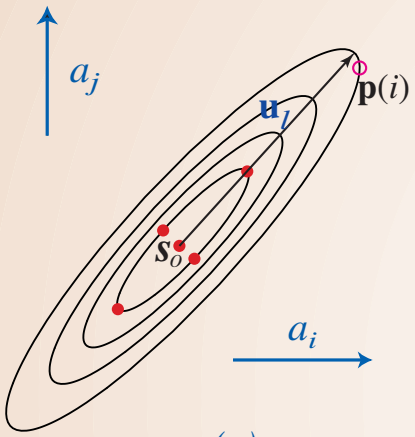

(a)
Original parameter basis

contours of constant χ^2_{global}
$\mathbf{u}_l$: *eigenvector in the l-direction*
$\mathbf{p}(i)$: *point of largest* a_i *with tolerance T*
s_0: *global minimum*

diagonalization and rescaling by the iterative method

- *Hessian eigenvector basis sets*

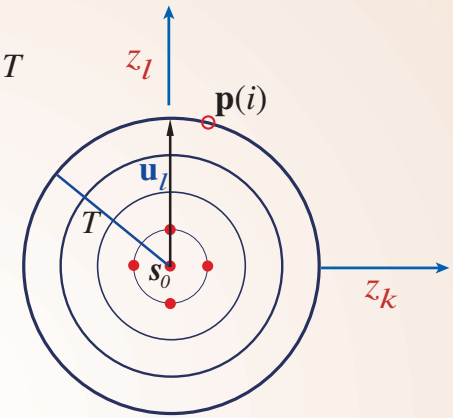

(b)
Orthonormal eigenvector basis

A hyperellipse $\Delta\chi^2 \leq T^2$ in space of N physical PDF parameters $\{a_i\}$ is mapped onto a hypersphere of radius T in space of N orthonormal PDF parameters $\{z_i\}$

Tolerance hypersphere in the PDF space

2-dim (i,j) rendition of N-dim (22) PDF parameter space

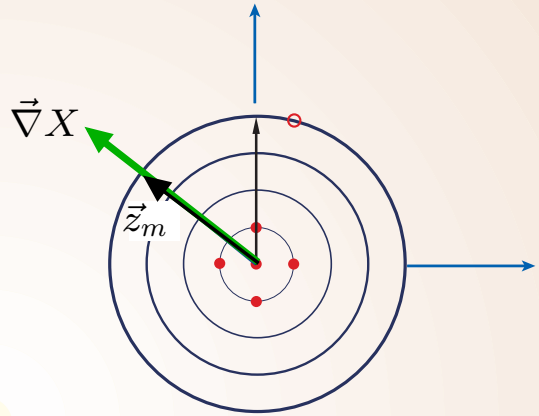

(b)
Orthonormal eigenvector basis

PDF error for a physical observable X is given by

$$\Delta X = \vec{\nabla} X \cdot \vec{z}_m = \left|\vec{\nabla} X\right| = \frac{1}{2}\sqrt{\sum_{i=1}^{N}\left(X_i^{(+)} - X_i^{(-)}\right)^2}$$

Tolerance hypersphere in the PDF space

2-dim (i,j) rendition of N-dim (22) PDF parameter space

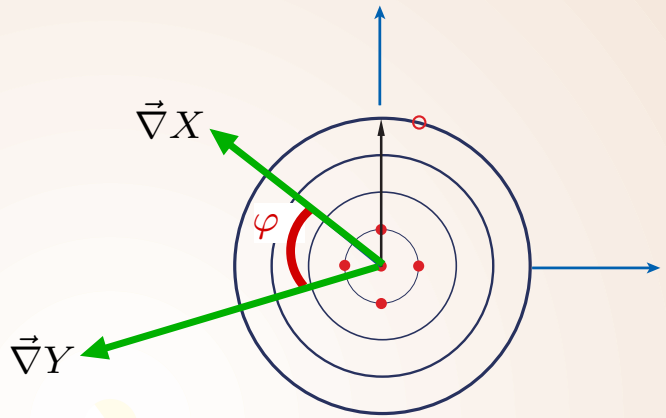

(b)
Orthonormal eigenvector basis

Correlation cosine for observables X and Y:

$$\cos\varphi = \frac{\vec{\nabla} X \cdot \vec{\nabla} Y}{\Delta X \, \Delta Y} = \frac{1}{4 \Delta X \, \Delta Y} \sum_{i=1}^{N} \left(X_i^{(+)} - X_i^{(-)} \right) \left(Y_i^{(+)} - Y_i^{(-)} \right)$$

Z, W, $t\bar{t}$ cross sections and correlations

Table: Total cross sections σ, PDF-induced errors $\Delta\sigma$, and correlation cosines $\cos\varphi$ for Z^0, $W^\pm$, and $t\bar{t}$ production at the Tevatron Run-2 (Tev2) and LHC, computed with CTEQ6.6 PDFs.

$\sqrt{s}$ (TeV)	Scattering process	$\sigma, \Delta\sigma$ (pb)	Correlation $\cos\varphi$ with Z^0 (Tev2)	$W^\pm$ (Tev2)	Z^0 (LHC)	$W^\pm$ (LHC)
1.96	$p\bar{p} \to (Z^0 \to \ell^+\ell^-)X$	241(8)	1	**0.987**	0.23	0.33
	$p\bar{p} \to (W^\pm \to \ell\nu_\ell)X$	2560(40)	**0.987**	1	0.27	0.37
	$p\bar{p} \to t\bar{t}X$	7.2(5)	-0.03	-0.09	-0.52	-0.52
14	$pp \to (Z^0 \to \ell^+\ell^-)X$	2080(70)	0.23	0.27	1	**0.956**
	$pp \to (W^\pm \to \ell\nu)X$	20880(740)	0.33	0.37	**0.956**	1
	$pp \to (W^+ \to \ell^+\nu_\ell)X$	12070(410)	0.32	0.36	**0.928**	**0.988**
	$pp \to (W^- \to \ell^-\bar{\nu}_\ell)X$	8810(330)	0.33	0.38	**0.960**	**0.981**
	$pp \to t\bar{t}X$	860(30)	-0.14	-0.13	**-0.80**	**-0.74**

Correlations with single-top cross sections

Table: Correlation cosines $\cos\varphi$ between single-top, W, Z, and $t\bar{t}$ cross sections at the Tevatron Run-2 (Tev2) and LHC, computed with CTEQ6.6 PDFs.

Single-top production channel	Correlation $\cos\varphi$ with Z^0 (Tev2)	$W^\pm$ (Tev2)	$t\bar{t}$ (Tev2)	Z^0 (LHC)	$W^\pm$ (LHC)	$t\bar{t}$ (LHC)
$t-$channel (Tev2)	-0.18	-0.22	**0.81**	**-0.82**	**-0.79**	0.56
$t-$channel (LHC)	0.09	0.14	-0.64	0.56	0.53	-0.42
$s-$channel (Tev2)	**0.83**	**0.79**	0.18	0.22	0.27	-0.3
$s-$channel (LHC)	**0.81**	**0.85**	-0.42	0.6	0.68	-0.33

$t\bar{t}$ production as a standard candle process

Uncertainties in $\sigma_{t\bar{t}}$ for $m_t = 171$ GeV

Type	Current	Projected	Assumptions
Scale dependence	11% (NLO)	$\sim 3-5\%$? (NNLO+resum.)	$m_t/2 \leq \mu \leq 2m_t$
PDF dependence	2%	1%?	1σ c.l.
m_t dependence	5% $\delta m_t = 2$ GeV	$< 3\%$ $\delta m_t = 1$ GeV	
Total (theory)	12%	$\sim 5\%$	
Experiment	8% (CDF)	5%?	

- Measurements of $\sigma_{t\bar{t}}$ with accuracy $\sim 5\%$ may be within reach; useful for monitoring of $\mathcal{L}_{LHC}$ in the first years, normalization of cross sections sensitive to large-x glue scattering, as well as for new physics searches *(reviewed by T. Han in arXiv:0804.3178)*

Updated theory estimates in Cacciari et al., arXiv:0804.2800; Moch, Uwer, arXiv:0804.1476

$\sigma(W^+)/\sigma(W^-)$

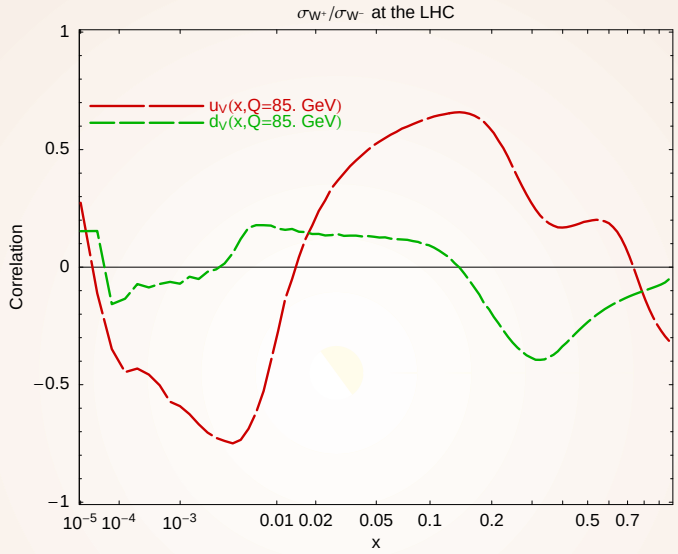

$\sigma(W^+)/\sigma(W^-) = 1.36 + 0.016$ (CTEQ6.6), 1.36 (MSTW'06NNLO), 1.35 (MRST'04NLO)

Combined HERA-1 data set on neutral-current DIS cross sections

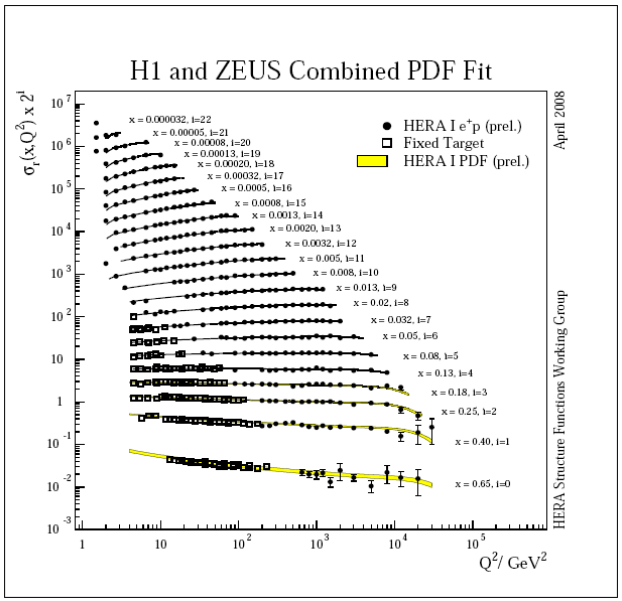

New HERA-I PDF fit predictions vs. H1/ZEUS combined data for NC e^+p.

Total uncertainties on the PDF fit predictions are included but can barely be resolved.

Averaging of the data leads to cross-calibration of H1 and ZEUS measurements, drastic reduction of systematic uncertainties

Gang Li, HERALHC workshop, 2008